NETZSCH

Proven Excellence.

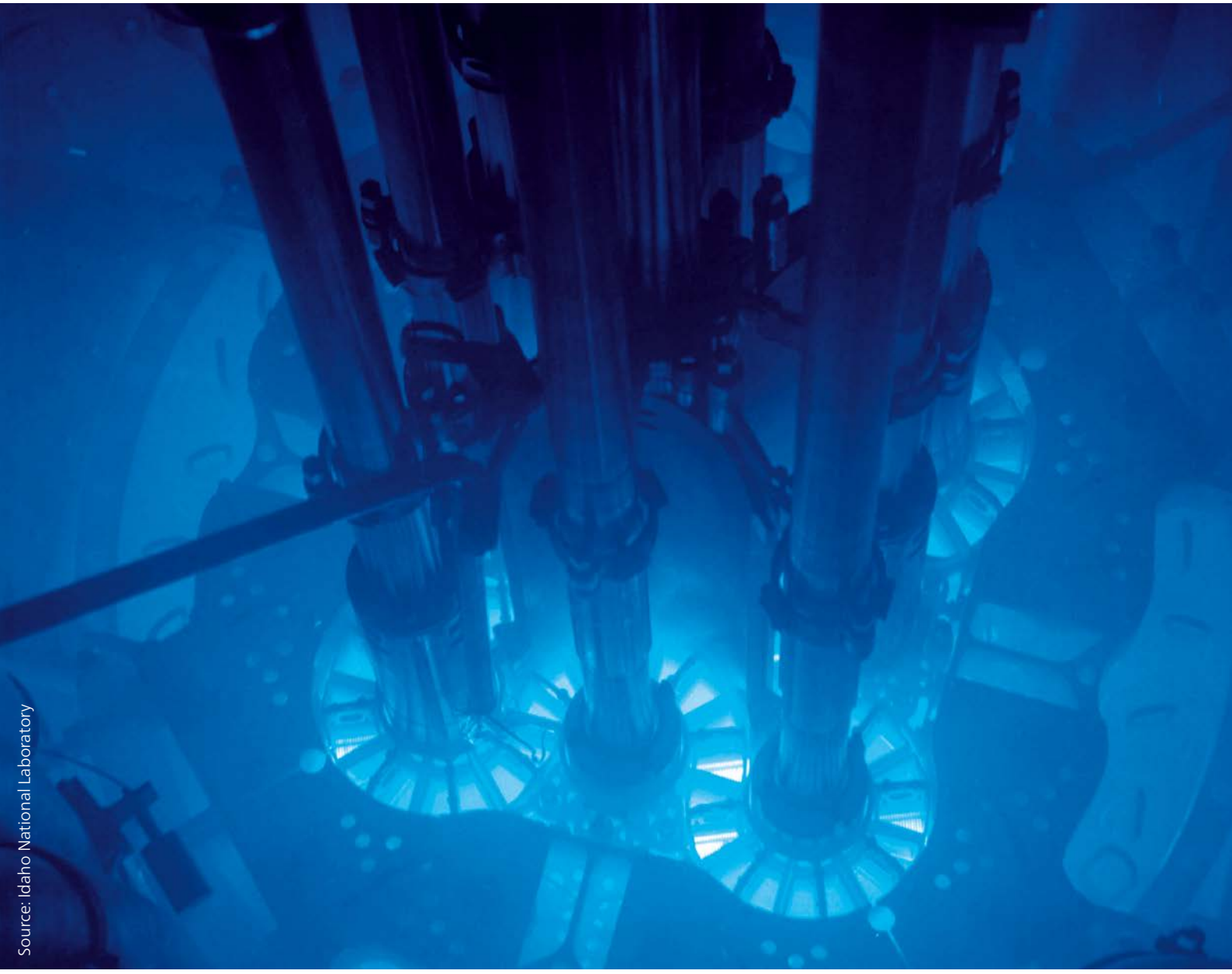

Source: Idaho National Laboratory

Characterization of Nuclear Materials

Methods, Instrumentation, Applications

Analyzing & Testing

Introduction

The world demand for electricity is projected to double by mid-century. Because of the ever-increasing price of fossil fuels and the associated environmental concerns such as carbon dioxide emissions, nuclear power generation is regaining popularity. Nuclear fuel is clean and relatively inexpensive compared to fossil fuels. It is in fact the only source of clean, sustainable and affordable energy which can meet current and near-term demands for electricity generation, if sufficient numbers of reactors of current and advanced design can be brought on line in a timely manner. In addition, the nuclear reactors of current design are safe and, save a natural disaster such as the magnitude 9 earthquake east of Japan and resulting tsunami, accidents are highly unlikely. In spite of the accident at the Fukushima nuclear power plant caused by the earthquake/tsunami, the strong resurgence – so-called renaissance – of nuclear power is expected to continue.

This renaissance has led to the formation of a multi-national cooperation called the Global Nuclear Energy Partnership (GNEP). Two of the stated aims of GNEP are to:

- develop a new generation of nuclear power plants – the so-called Generation IV systems (GEN IV) in which six different reactor types are under consideration (both thermal and fast reactors), and
- reduce waste by recycling used nuclear fuel using new technologies.

The history of commercial nuclear power generation reaches back to the mid-60s. The Generation III+ reactors now under development and the GEN IV reactors under consideration are of unique design with respect to safety, performance and economics. The GEN IV reactors include the Very High Temperature Reactor (VHTR), the Sodium-cooled Fast Reactor (SFR) and perhaps the most unique, the Molten-Salt Reactor (MSR). Many of these reactors will contain unique fuel systems and reactor materials.

Generation I	Generation II	Generation III	Generation III+	Generation IV
Early Prototype Reactors	Commercial Power Reactors ▪ LWR-PWR, BWR ▪ CANDU ▪ AGR	Advanced LWRs	Evolutionary Designs Offering Improved Economics for Near-Term Deployment	▪ Highly Economical ▪ Enhanced Safety ▪ Minimal Waste ▪ Proliferation Resistant

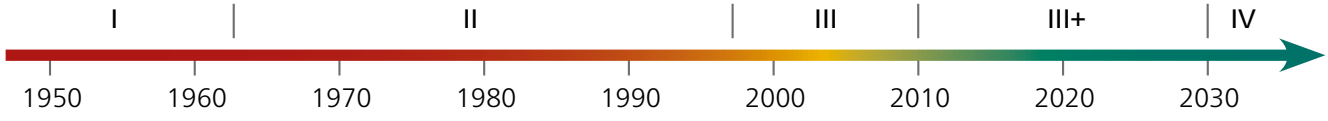

Time line for reactor development

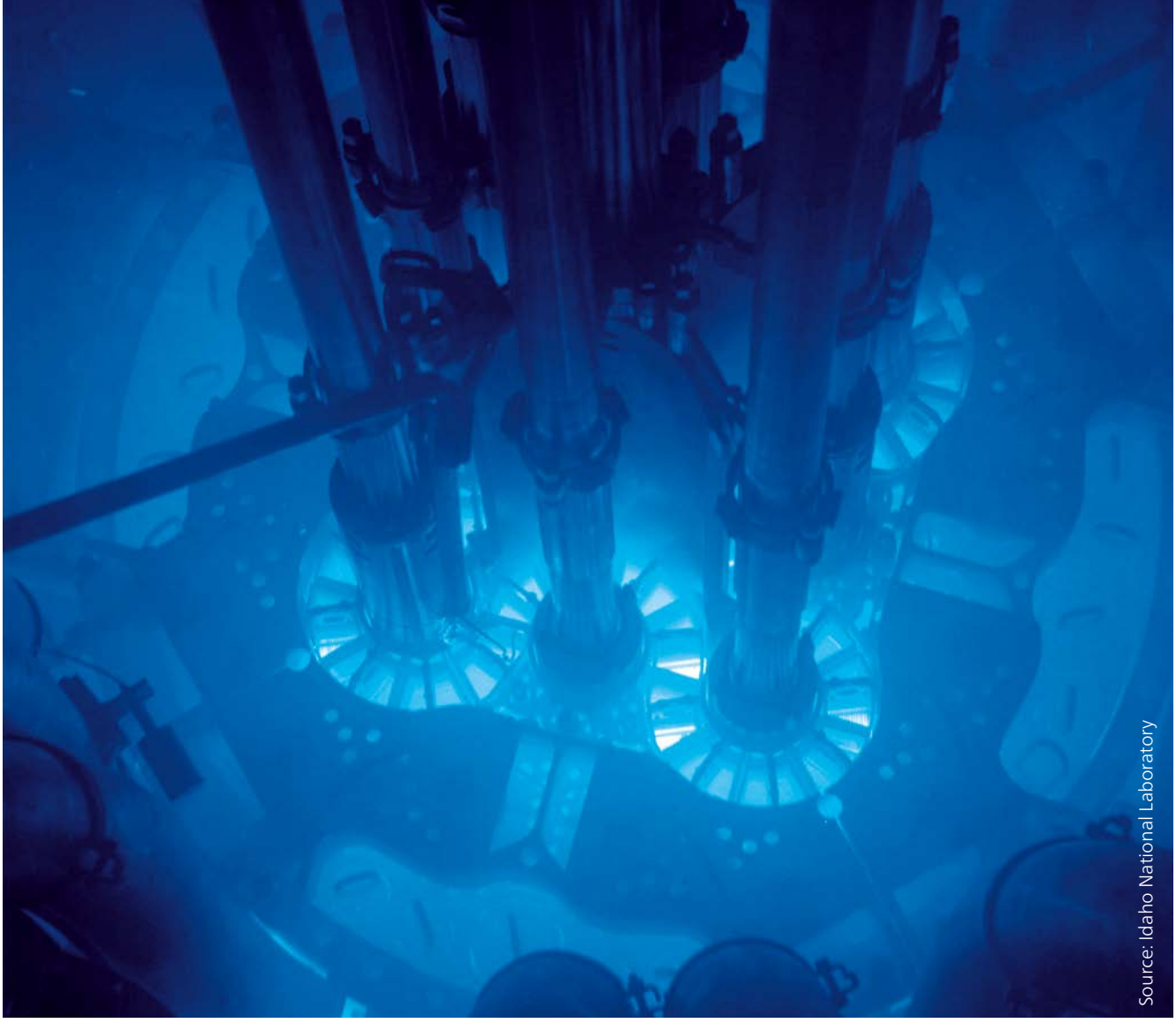

Soure: Idaho National Laboratory

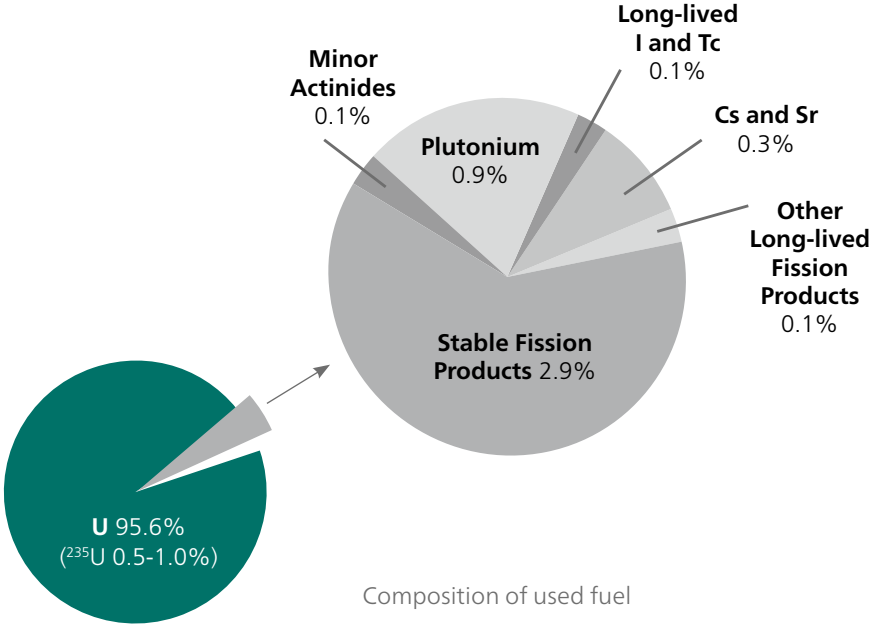

Composition of used fuel

The major concern with nuclear power generation today is the safe disposal of used fuels. Because of storage-related problems, recycling of used fuel is of paramount importance. Fuel recycling is not a new concept. In fact, used fuel from light-water reactors (LWR) has been reprocessed into $(U,Pu)O_2$ – so-called MOX fuel – for some time by various countries. This is economically feasible because spent fuel contains not only fission products and minor actinides such as Americium, Neptunium and Curium, but a large percentage of fissile Uranium and Plutonium isotopes as well.

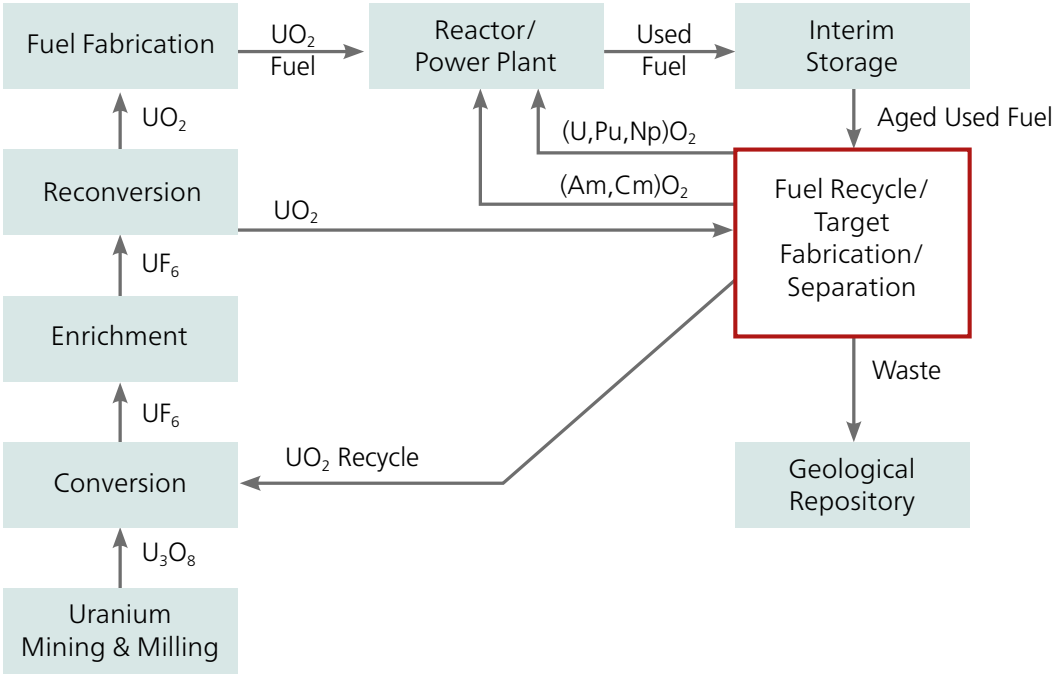

Closed fuel cycle with front end processing of UO_2 and back end recycling/target fabrication

It has been estimated that the effective capacity of geological repositories can be increased greatly if the long-lived minor actinides such as those mentioned above plus Pu (transuranics) are separated and fabricated into the reprocessed fuel or targets for transmutation/consumption. Several concepts have been proposed to realize this, some of which utilize fast reactors and others thermal reactors.

In addition, studies have shown that significant reductions in repository heat and radiotoxicity loads can be realized by placing used fuel in interim storage for a few years to allow short-lived fission products such as Cs-137 and Sr-90 to partially decay prior to separation.

Interim storage also reduces the problems associated with reprocessing fuel containing Cm, but also increases the content of high-vapor-pressure Am-241 due to the β-decay of Pu-241.

Of course, a prerequisite for the successful design of any new reactor or fuel system as well as modernization of the existing reactor fleet is the accurate knowledge of the thermophysical properties for the materials of interest. This will necessitate the measurement of the thermophysical properties for fresh, reprocessed and used fuels as well as irradiated and unirradiated reactor component materials.

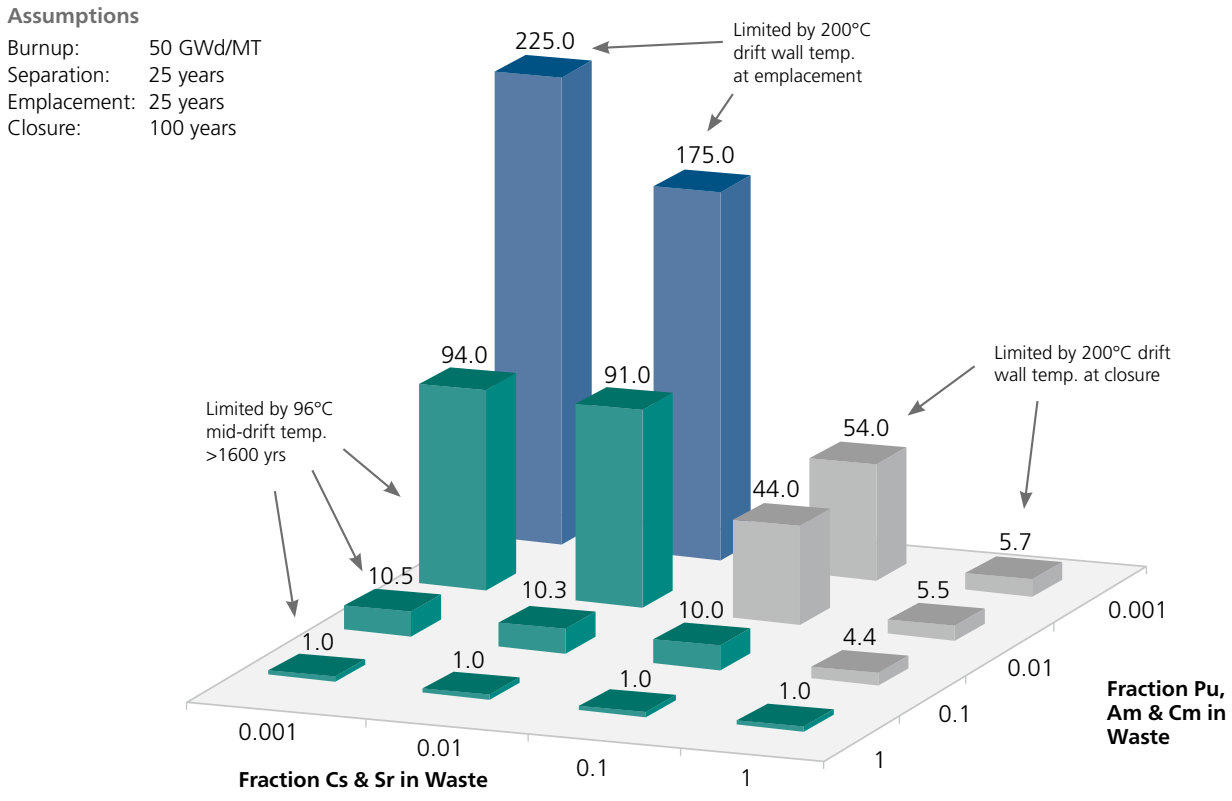

The calculated increase in repository capacity as a function of reduced Cs, Sr, Pu, Am and Cm content with separation after 25 years "Separations and Transmutation Criteria...", Wigeland, et al., Nuc. Tech., 2006

Property measurements on fission products and/or their surrogates, glasses, containment components and geological materials associated with long-term isolation in repositories are also of paramount importance. The properties of interest include but are not limited to the thermal conductivity, thermal diffusivity, specific heat, transformation energetics, thermal expansion, bulk density, solidus/liquidus temperatures and O/M ratio. Clearly, measurement of these properties on the materials mentioned above will necessarily be carried out in glovebox and hot cell environments as well as in cold facilities.

Over the past few years NETZSCH-Gerätebau GmbH has become the leading supplier of thermal analysis and thermophysical properties instrumentation to the nuclear industry. This is because our instruments are reliable, robust, accurate and easy to use. All of these attributes are necessary for instruments operating in harsh environments such as gloveboxes and hot cells. Further, the modular design of our instruments makes them ideally suited for incorporation into these environments. Finally, the costs of operating in hot cells and gloveboxes are extremely high, making downtime critical. Our exemplary global service is therefore one more reason for our success.

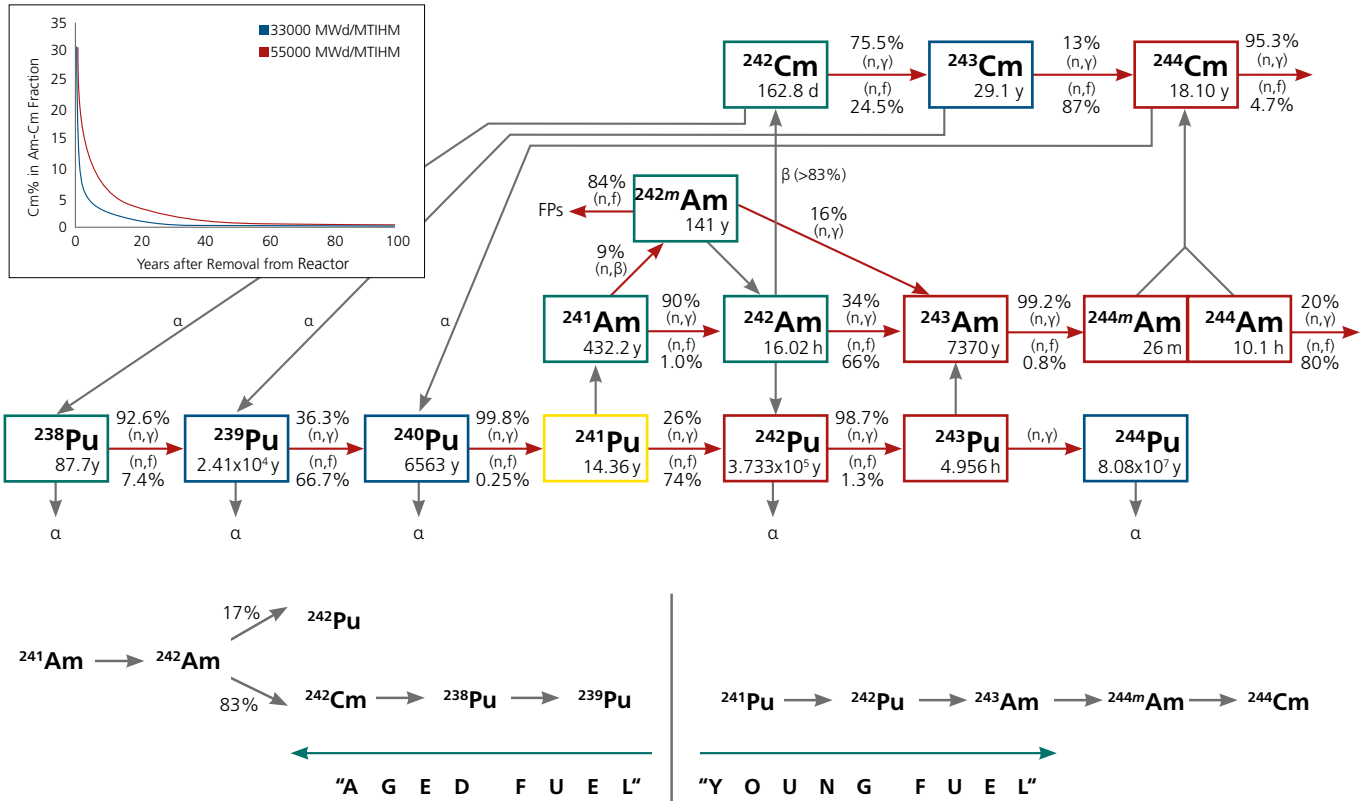

Transmutation Benefits of Older Fuel
"Closed Nuclear Fuel Cycle…", Collins, et al., Atalante 2008 Int. Conf., 2008

Thermophysical Properties

Introduction

Thermophysical properties can be divided into two categories – transport and thermodynamic. Transport properties include, but are not limited to, thermal conductivity, electrical resistivity and thermal diffusivity. (Actually, thermal diffusivity is a hybrid transport/thermodynamic property.) Thermodynamic properties include specific heat, transition energetics and thermal expansion (bulk density).

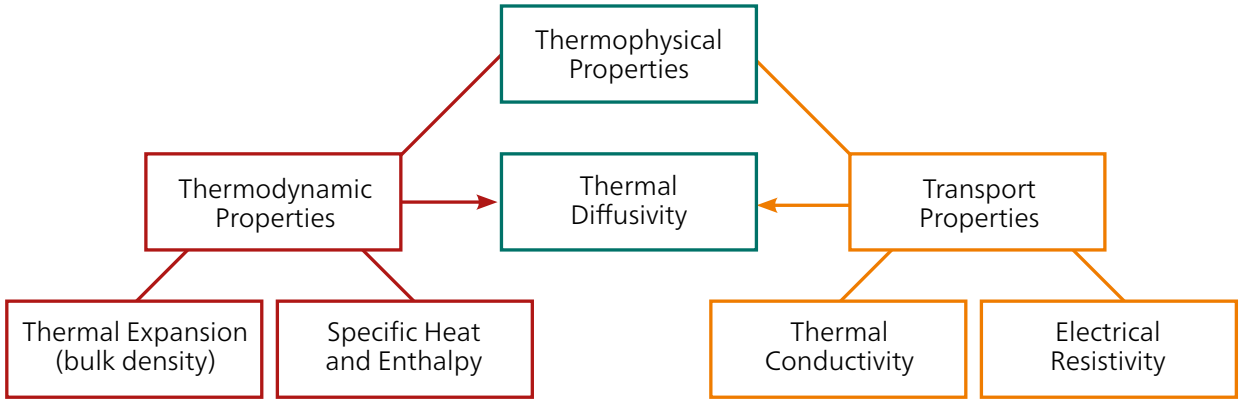

Classification of some thermophysical properties

Thermal Conductivity

The thermal conductivity is perhaps the single most important thermophysical property and is paramount to the design of any system operating at elevated or sub-ambient temperatures. It consists of a lattice and/or electronic component, depending on the material (other components are also possible). It is well known in the nuclear industry that the thermal conductivity controls:

- temperature gradients in fuel
- efficiency of cladding and heat exchangers
- ability of geological repositories and container material to dissipate heat
- heat transfer in multi-layer fuel systems, e.g. TRISO.

The complete list is quite long. The thermal conductivity is greatly affected by corrosion, hydriding, fouling, O/M ratio, fission product carry-over, irradiation damage, composition, porosity, etc. The thermal conductivity/thermal diffusivity of almost all nuclear materials is most efficiently measured by the laser flash technique (LFA). LFAs can readily be incorporated into gloveboxes and hot cells with the appropriate modifications.

Specific Heat and Transition Energetics

The capacity of a material to store energy is governed, in part, by the specific heat (sensible heat). It is made up of lattice, electronic and defect components, depending on the material. This property is required for design of any transient heat transfer process. It is also used to quantify surface oxidation/reduction and O/M ratio (defects) of fuels during processing. In some cases, the specific heat can be used as an indicator of the extent of damage in post irradiation examination (PIE), e.g. stored energy. It is also required to calculate the thermal conductivity from thermal diffusivity data.

Transition energetics (latent heat) are required to characterize solid-solid transitions, melting/solidification and decomposition. Both specific heat and transition energetics are most accurately and efficiently measured by differential scanning calorimetry (DSC). The specific heat can also be measured by the laser flash technique, albeit with reduced accuracy and only with a reduced number of data points. (With DSC, generation of a quasi-continuous set of temperature-dependent specific heat data is standard.) With the required expertise, DSCs can readily be adapted for hot work.

Thermal Expansion

Thermal expansion can be made up of lattice, electronic, magnetic and vacancy/interstitial components, depending upon the material and temperature. Thermal expansion data are key to both reactor and fuel design. For example, it is necessary for quantification of:

- fuel swelling during irradiation
- fuel/coating compatibility (e.g. UO_2/graphite/SiC or ZrC)
- abrasion and corrosion coating/substrate compatibility
- densification during sintering
- thermal expansion coefficients
- volume change during melting/solidification
- bulk density

and, as stated earlier, the data can be used to determine solidus and liquidus temperatures. By far the most versatile, accurate and economical technique to measure thermal expansion is pushrod dilatometry. Dilatometers are well suited for glovebox/hot cell work.

Solidus and Liquidus Temperatures

Solidus and liquidus temperature as well as melting temperature data are necessary to establish safe reactor operating conditions and to model accident scenarios such as loss of coolant. These temperatures are greatly affected by impurities, radiation damage, O/M ratios, burnup and, of course, composition. Surprisingly, solidus/liquidus temperatures are notoriously difficult to measure accurately. DSC is the technique most often employed for these measurements, but care must be taken to avoid undercooling during solidification (especially critical for metal alloys). Sample time constants and temperature ramp rates must be carefully considered. Solidus/liquidus temperatures of most metal alloys can also be measured by the laser flash technique (by utilization of thermal conductivity/thermal diffusivity data) and dilatometry can be used for conductors and insulators alike. For materials that melt at ultra-high temperatures, thermal arrest is sometimes employed using optical pyrometers for the temperature measurement. All things considered, DSC is the most versatile and accurate method.

Mass Change and Evolved Gases

Temperature-dependent mass change coupled with evolved gas analysis provides valuable information to help quantify: O/M ratio, out-gassing during fuel processing, corrosion, reduction, volatile fission products/actinides during vitrification, impurities remaining from the separation process, etc. A thermogravimetric analyzer (TGA) or simultaneous TGA-DSC (STA) instrument coupled to a quadrupole mass spectrometer (QMS), either directly or by a heated transfer line, or a TGA or STA coupled to an FT-IR via a heated transfer line are widely employed for these types of analysis. As with the other techniques previously discussed, these instruments can easily be modified for hot work.

INSTRUMENTATION

Flash Technique

The flash method is the fastest and most accurate way of measuring the thermal diffusivity (⇨ thermal conductivity). It has been estimated that 80-85% of all thermal diffusivity/ thermal conductivity measurements are carried out using this technique. This is because of:

- easy sample preparation: coin-sized disk or square/rectangle (can be even smaller)
- flexibility: measurements on solids, liquids, pastes, powder and laminate samples
- small sample size: ideal for fuels/irradiated materials
- fast measurement times: due to small sample size
- high accuracy: usually better than 5%
- wide thermal diffusivity/thermal conductivity range: approx. 0.01 to 1000 W/m·K
- wide temperature range: -125°C to 2800°C

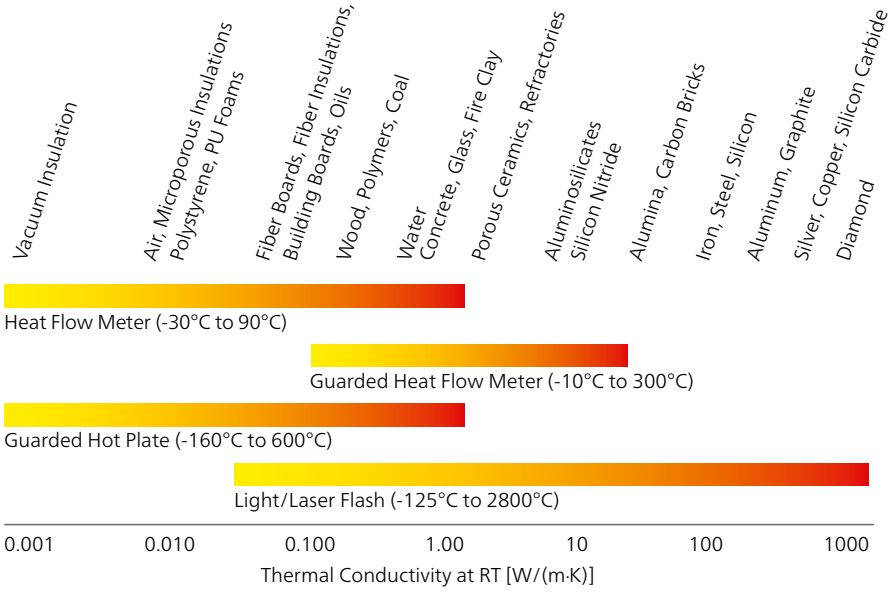

Comparison of the flash method with other techniques utilized in NETZSCH instruments as well as approximate room temperature thermal conductivity ranges of several types of materials.

As shown on the right, the front surface of a sample is heated by a short energy pulse (xenon or laser) and the time-dependent temperature rise on the rear surface is measured by an IR detector. From a plot of T / T_{max} (or V / V_{max}) vs half-time, the thermal diffusivity of a perfectly insulated sample at one half-time is given by:

$$a = 0.1388\ l^2/t_{½}$$

where

a = thermal diffusivity (mm^2/s)
l = sample thickness (mm)
$t_{½}$ = half-time (s)

There are several sophisticated models to correct for heat loss (non-adiabatic conditions) and the finite pulse width of the energy source.

Using the measured thermal diffusivity values, the thermal conductivity is calculated by:

$$\lambda(T) = a(T) \cdot c_p(T) \cdot \rho(T)$$

where

λ = thermal conductivity ($W/m \cdot K$)
ρ = bulk density (g/m^3)
C_p = specific heat ($J/g \cdot K$)

The bulk density can be obtained from thermal expansion data, and the specific heat by either the LFA or a DSC.

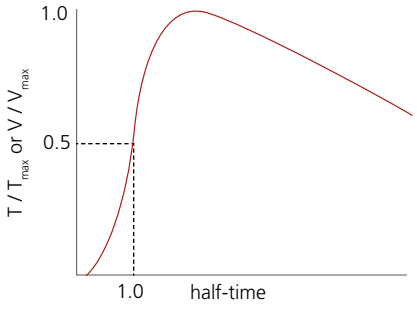

Experimental data

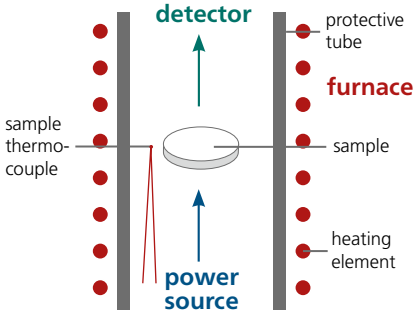

Flash technique

Light/Laser Flash Analysis

The NETZSCH LFAs cover almost the entire range of temperatures and materials of interest to the nuclear industry. For convenience, some of the specifications are summarized in the table below.

Model	Temperature Range	Atmosphere	Energy	Detector
LFA 717	-100°C to 500°C	inert, oxid.	Xenon flash	InSb / MCT
LFA 717 *HT*	RT to >1250°C	inert, oxid., vac.	Xenon flash	InSb
LFA 427	-120°C to 2800°C	inert, oxid., red., vac., corr.	Laser	InSb / MCT

LFA 717 *HyperFlash*® Series

The LFA 717 *HyperFlash*® series is based on a Xenon flash with a compact design. The low-temperature version covers the temperature range from -100°C to 500°C. A variety of cooling options allow for measurements to be carried out across the full temperature range of the instrument without having to change either the furnace or the detector. The integrated automatic sample changer (ASC) allows for unattended analyses on up to 16 samples.

The high-temperature version, LFA 717 *HyperFlash*® *HT*, operates between RT and >1250°C; the ASC handles up to 4 specimens.

LFA 717 *HyperFlash*® *HT* and LFA 717 *HyperFlash*®

LFA 427

The 427 is the most powerful and versatile LFA system for research and development as well as all applications involving the characterization of standard and nuclear materials.

The LFA 427 guarantees high precision and reproducibility, short measurement times and defined atmospheres over a temperature range of -120°C to 2800°C. Special holders for liquid, fiber, paste, powder and laminate samples are available. Even fuel fragments can be tested.

The system is vacuum tight to 10^{-5} mbar. The variable laser power and pulse width functions make it easy to optimize test parameters.

LFA 427 modified for hot cell operation

Differential Scanning Calorimetry (DSC)

Heat flux DSCs function by measuring the temperature difference (voltage difference) between a sample and a reference while being heated or cooled at a constant rate. The resulting signal is proportional to the mass × specific heat (sensible heat) plus the energy associated with any phase change, etc. (latent heat). This signal is converted to actual physical quantities through calibration using melting point standards having well-defined heats of fusion or specific heat standards with well-established and reproducible temperature-dependent specific heat values. This is typically referred to as a sensitivity calibration. The signal generated by a heat flux DSC is shown here.

The temperature-dependent specific heat is obtained by running a baseline (empty crucibles), standard and sample scan. Using these data the specific heat is calculated by the so-called ratio method where the specific heat of the sample is given by:

$$C_{p,s} = C_{p,std} \frac{m_{std}}{m_s} \frac{\mu V_s - \mu V_{BL}}{\mu V_{std} - \mu V_{BL}}$$

where

$C_{p,s}$ = sample specific heat [J/(g·K)]
$C_{p,std}$ = standard specific heat [J/(g·K)]
m_s = sample mass [g]
m_{std} = standard mass [g]
μV_s = sample scan signal
μV_{std} = standard scan signal
μV_{BL} = baseline scan signal

The resulting specific heat curve will also include any latent heat due to phase transitions, etc. In the temperature region of a phase transition the result is typically referred to as apparent specific heat. The resulting peak in the specific heat curve can then be integrated to give the transition energy, Δh (J/g). Finally, the onset and end of the latent heat peaks can be used to define the solidus and liquidus temperatures as long as time constants and undercooling are given proper consideration.

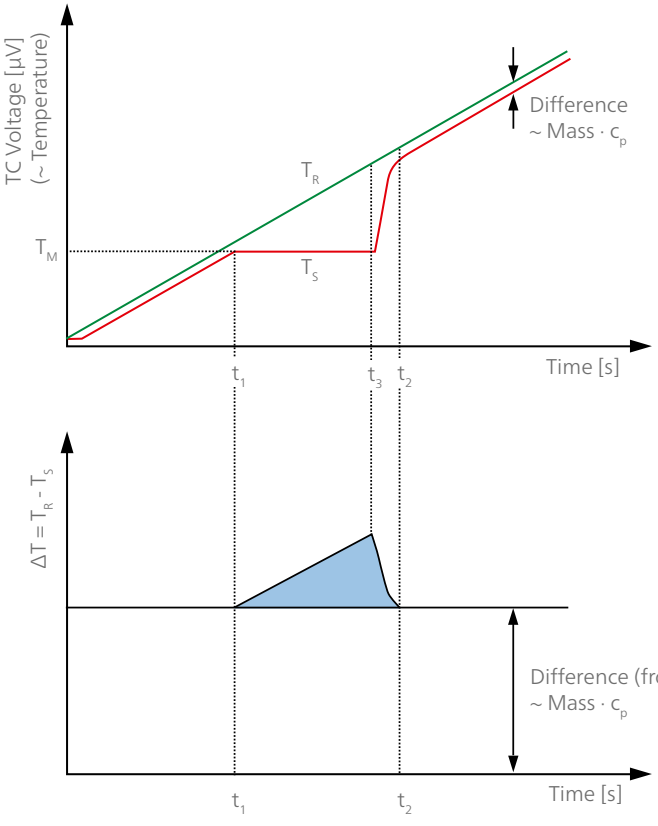

Reference signal
Sample signal
T_M Transition temperature
Area A
~ Transition enthalpy
T_R Temperature Reference
T_S Temperature Sample
t_1 Onset
t_2 Endset
t_3 Peak

Signal generation in a heat flux DSC

The NETZSCH DSC 500 *Pegasus*® covers most applications of interest to the nuclear industry. An overview of some of the specifications is given in this table.

Model	Temperature Range	Atmosphere	Vacuum	Sensor Types
DSC 500	-150°C to 2000°C	inert, oxid., red., vac., corr., humid	10^{-4} mbar	E, K, S, B, W-Re

DSC 500 *Pegasus*®

The DSC 500 *Pegasus*® has a temperature range of -150°C to 2000°C and are vacuum-tight down to 10^{-4} mbar. Eight different furnaces are available and, when equipped with a double hoist, 2 furnaces can be mounted simultaneously. There are 13 different user-exchangeable *Quick-Connect* plug-in sensors which allow optimization of sensitivity and time constants.

The DSC 500 *Pegasus*® was designed specifically for high-temperature specific heat measurements. Accuracies in the range of ±2.5% can be obtained for most materials over the temperature range of -150°C to 1400°C for specific heat and better than 2.0% for latent heat over the temperature range of -150°C to 1650°C.

Evolved gases can also be identified and quantified (with optional *Pulse*TA® unit) by coupling the DSC to an MS, GC-MS and/or an FT-IR via a heated furnace adapter head and heated transfer line. Special options for corrosive gases are also available.

An automatic sample changer is available for the DSC 500 *Pegasus*®, but is not generally recommended for glovebox/hot cell operation.

This unit is widely used in the nuclear industry in both cold and hot applications. The glovebox/hot cell versions are equipped with special sample loading mechanisms and sample carrier adjustment systems to facilitate operation. These special configurations have reduced footprints with separate electronics and MFCs located outside the glovebox or hot cell.

DSC 500 *Pegasus*® with automatic sample changer

Dilatometry (DIL)

Pushrod dilatometers measure, via an LVDT, the thermal expansion of a sample while it is being heated at a constant rate or held isothermally (with the exception of non-linear rates in rate-controlled sintering studies). The voltage signal is proportional to the expansion of the sample. This raw signal is converted to the length change by calibrating the instrument using a standard with a well-defined and reproducible thermal expansion.

The temperature-dependent length change is used to calculate the coefficient of linear expansion, α, i.e.:

$$\alpha = \frac{1}{L_0}\frac{\Delta L}{\Delta T} = \frac{1}{L_0}\frac{(L_2 - L_1)}{(T_2 - T_1)}$$

where

L = length (mm)
L_0 = initial length (mm)
T = temperature (°C)

The volumetric expansion for an isotropic material is then calculated by:

$$\frac{\Delta V}{V_0} \approx 3\alpha\Delta T$$

where

V = volume (cm^3)
V_0 = initial volume (cm^3)

Thus, the instantaneous temperature-dependent bulk density, ρ, for an isotropic material can be calculated using:

$$\rho = \frac{m}{V} \approx \frac{m}{V_0(1 + 3\alpha\Delta T)}$$

where

m = instantaneous mass (g).

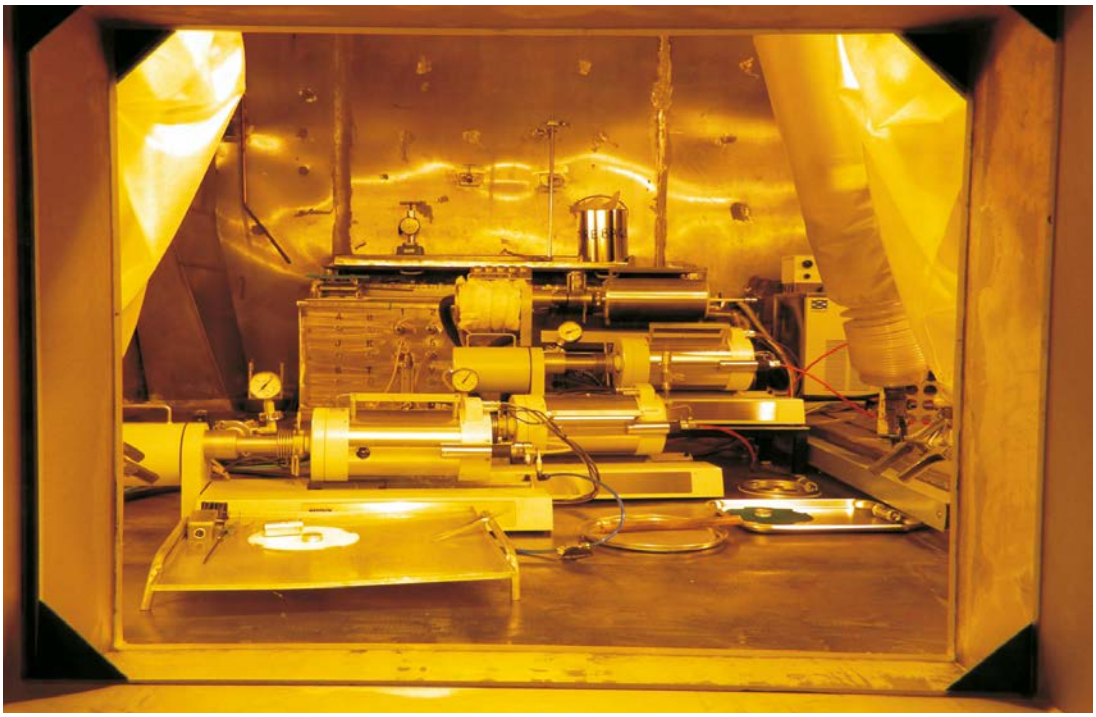

Four modified dilatometers operating in a hot cell

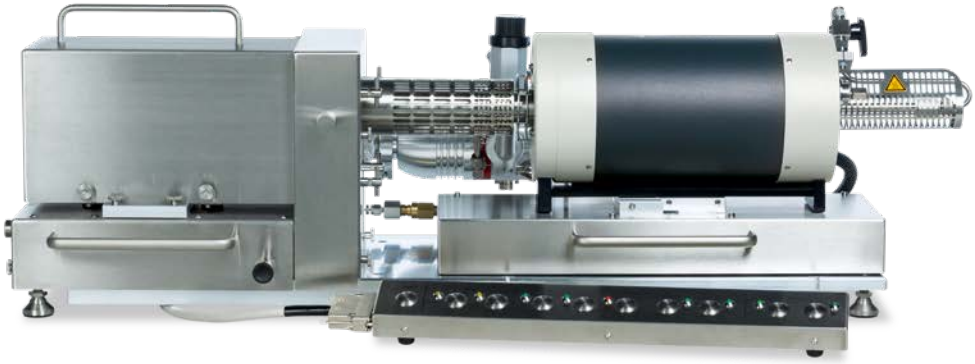

DIL *Expedis Supreme* Glovebox Version with separate control panel (option) for use inside the glovebox

NETZSCH DIL 502 Series

NETZSCH manufactures various unique horizontal dilatometer models which operate over a temperature range of -260°C to 2800°C.

Featuring a new opto-electrical displacement system, the *Expedis* dilatometers series offers highest resolution associated with an unmatched measuring range which is higher up to a factor 10 compared to traditional dilatometers. Highest reproducibility is given by the friction-free construction. The controlled contact force during the entire measurement allows for tests on small, delicate, fragile or foamed samples without the risk of non-reproducible deformation. Extremely small forces are adjustable on green bodies or soft samples.
The E and ED dilatometers stand out by their extreme temperature range. The transducers housings are thermostatted and have Invar LVDT mounting systems. This ensures that the length signal is not disturbed by the furnace or fluctuations in the room, glovebox or hot cell temperature.

These dilatometers (except the ED) can be equipped with different user-exchangeable furnaces. All models are vacuum-tight down to 10^{-5} mbar and 10^{-4} mbar, respectively. Graphite, Al_2O_3 and fused silica sample carriers and pushrods with different sample thermocouple types are available. Special holders for liquid metals, pastes, powders, fibers and thin films can also be delivered.

Software options such as c-*DTA*®, RCS, density and thermokinetics allow for calculation of phase transitions, measurement of densification under variable heating rate conditions, calculation of bulk density from linear expansion data for isotropic samples and kinetic evaluation during phase transitions and sintering, respectively. Using special sample holders, the solidus and liquidus temperatures can also be determined.

The small footprint and horizontal design of the NETZSCH dilatometers make them ideal for incorporation into gloveboxes/hot cells.

The NETZSCH dilatometers cover almost all conceivable nuclear applications.
For convenience, some of the specifications are summarized in this table.

Model	Temperature Range	Atmosphere	Δl Resolution	Types
DIL 502 *Expedis Supreme*	-180°C to 2800°C	inert, oxid., red.,vac.	0.1 nm	single/dual sample/ differential
DIL 502 *Expedis Select*	-180°C to 2000°C	inert, oxid., red.,vac.	1 nm	single/dual sample/ differential

Thermomechanical Analysis (TMA)

Thermomechanical Analysis (TMA) determines dimensional changes of solids, liquids or pasty materials as a function of temperature and/or time under a defined mechanical force (DIN 51 005, ASTM E831, ASTM D696, ASTM D3386, ISO 11359 – Parts 1 to 3). It is closely related to Dilatometry, which determines the length change of samples under negligible load (DIN 51 045).

Irrespective of the selected type of deformation (expansion, compression, penetration, tension or bending), every change of length in the sample is communicated to a highly sensitive inductive displacement transducer (LVDT) via a push rod and transformed into a digital signal.

The force imparted to the sample is generated electromagnetically. This guarantees a quick response time for experiments with a changing load, e.g. tests on creep behavior. A highly sensitive force sensor (digital resolution < 0.01 mN) continuously measures the force exerted via the push rod and readjusts it automatically. The force can be applied as a single pulse or as continuous modulation at frequencies up to 1 Hz. The force and displacement signals are measured simultaneously.

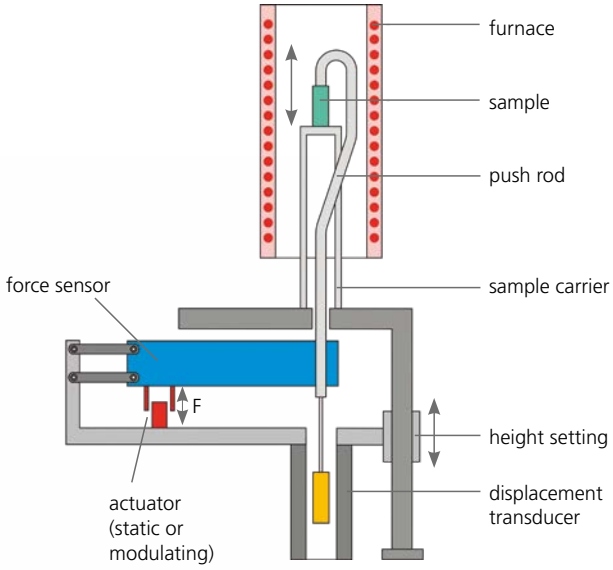

Thermomechanical Analysis (TMA)

Standard TMA 512 *Hyperion*®
with double furnace hoist

TMA 512 *Hyperion*® Series

The NETZSCH TMA is a vertical system and is available in a *Select* and *Supreme* version. Both models are vacuum tight with thermostatted LVDT housings and Invar mounting systems, making them ideal for the measurement of low CTE materials because the measurement signal is not disturbed by fluctuations in the room, glovebox or hot cell temperature. Both the *Select* and *Supreme* are available with a double furnace hoist which allows two furnaces to be mounted simultaneously (the -150°C to 1000°C steel furnace and the RT to 1500°C/1600°C SiC furnace). These furnaces are interchangeable with the NETZSCH STA 509 and DSC 500 series. Integrated software-controlled MFCs mean that sample purge gases can be switched or mixed (to control e.g. PO_2) as many times as necessary during the measurement.

Sample holders for expansion, penetration, tension and 3-point bending are available in Al_2O_3 or fused silica and are easily exchangeable. Further sample containers for powders, liquids, pastes and molten metals are available in several different materials.

The vertical design of the TMA 512 makes it ideal for coupling to an MS, GC-MS and/or FT-IR (chimney effect) and for glovebox/hot cell operation after, of course, the appropriate modifications such as separation of electronics, MFCs, etc.

As with the dilatometers, software options for c-*DTA*®, RCS, density and thermokinetics allow calculation of phase transitions, densification, calculation of bulk density, etc. Further, determination of visco-elastic properties from measurements using variable force is possible.

The NETZSCH TMAs are suitable for most nuclear applications.
For convenience, some specifications are shown here.

Technical Data	TMA 512 *Select*	TMA 512 *Supreme*
Max. sample length	30 mm	30 mm
Temperature range	-70°C to 1500°C/1600°C (2 furnaces)	-150°C to 1600°C (5 furnaces)
Atmosphere	inert, oxid., red., vac., corr., hydrogen	inert, oxid., red., vac., corr., humid plus hydrogen
Measuring range	± 2.5 mm	± 2.5 mm
Dig. resolution (length)	0.125 nm	0.125 nm
Force range	0.001 N to 3 N in steps of 0.02 mN (tension or pressure)	0.001 N to 4 N in steps of 0.02 mN (tension or pressure)
Dig. resolution (force)	< 0.01 mN	< 0.01 mN
Modulated force	optional	Up to 1 Hz
Final vacuum	$< 10^{-4}$ mbar	$< 10^{-4}$ mbar
Gas connections	Protective gas, 2 purge gases, 1 additional	Protective gas, 2 purge gases, 1 additional
Mass flow controller (MFC)	Optional	Standard

Thermogravimetric Analysis (TGA)
Evolved Gas Analysis (EGA)

TGAs measure the mass change of a sample during heating/cooling or in an isothermal phase via a sensitive microbalance. In systems in which the balance is located on top, the sample crucible is suspended in the furnace by a wire or rod. Instruments with such an arrangement are generally referred to as "hang-down" systems. If the balance is located below the furnace, the sample crucible sits on a sensor at the terminal end of a ceramic rod. These systems are commonly referred to as "top-loading". Some instruments make use of a horizontal design.

When TGA is coupled with DSC, simultaneous measurement of mass change and energetics (simultaneous thermal analysis – STA) with one instrument is possible. The advantage of this is that both the mass change and energetics are measured simultaneously on one sample so that the test conditions, e.g. gas flow rate, gas partial pressure, heating rate, temperature, etc. are identical. The rate of mass change is calculated from the mass signal.

If the STA is coupled to a QMS, GC-MS and/or an FT-IR, the mass change, energetics and evolved gases are measured simultaneously. Of course, this is ideal because the TGA and DSC tell us how much, while the evolved gases tell us what and, generally, why.

STAs can also be run in the so-called rate controlled mass change mode. In this case, the sample is not heated at a constant rate, but in such a fashion as to produce a constant rate of mass change. This is ideal for cases where high rates of mass loss can cause sample damage and/or skew the results, e.g., binder burnout during sintering of technical ceramics or powder metals.

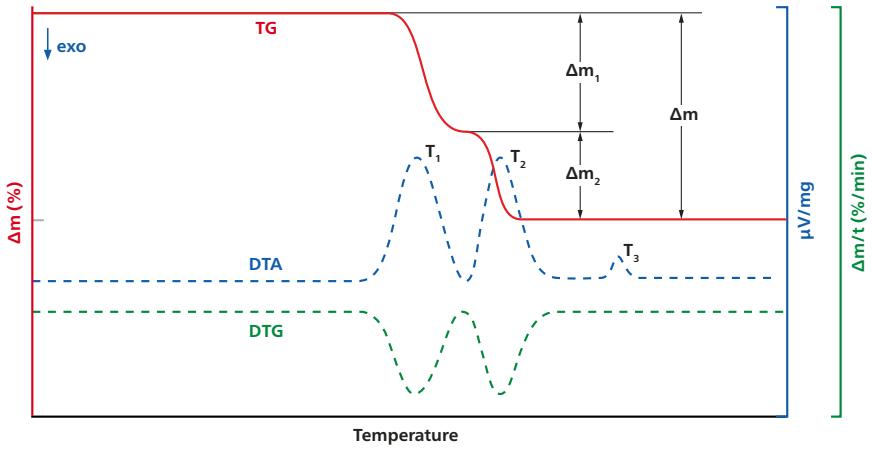

Measured and calculated STA curves

STA/EGA Systems

NETZSCH produces 3 different STA systems which cover a temperature range of 2000°C and 2400°C, respectively. There are 12 unique furnaces available and 16 different user-exchangeable *Quick-Connect* plug-in sensors which allow sensitivity/time constant optimization. The balances are all top-loading and purge gases flow from the bottom and exit at the top of the furnace along with the evolved gases. This arrangement is ideal for EGA work (chimney effect). The balances have high capacities and digital resolutions (see below). The units are all vacuum tight, making them well suited for work requiring controlled atmospheres. The STAs have excellent long-term stability (low drift) because the balance chambers are thermostatted to isolate the balance from fluctuations in glovebox/hot cell temperatures. The vacuum-tight design and long-term stability make the NETZSCH STAs ideal for corrosion and O/M studies. An optional water vapor furnace and generation system is an additional advantage for corrosion studies.

The NETZSCH STAs can be coupled to EGA systems (e.g., MS, GC-MS, FT-IR) via a heated adaptor head and heated transfer line or, in the case of the MS, directly via *SKIMMER* technology.

A well-defined quantity of gas can be injected into the STA via a *Pulse*TA® unit. This permits calibration of the EGA system so that the gases released from the sample can not only be identified, but quantified as well.

STA 509 *Jupiter*® coupled to a QMS 505 *Aëolos* via a capillary

The NETZSCH STA/EGA systems handle almost all nuclear applications.
For convenience, some system specifications are summarized below.

Model	Temperature Range	Atmosphere	Digital Resolution
STA 509 *Jupiter® Supreme*	-150°C to 2000°C	inert, oxid., red., vac., corr., humid	0.1 µg
STA 509 *Jupiter® Select*	-150°C to 2400°C	inert, oxid., red., vac., corr., humid	0.1 µg
STA 509 *Jupiter® Classic*	RT to 1600°C	inert, oxid., stat., vac., dyn.	< 2.0 µg

SKIMMER Coupling

A mass spectrometer can be directly coupled to the STA 449 ***F3*** *Jupiter*® via *SKIMMER* technology which utilizes a unique supersonic jet gas transfer system. The *SKIMMER* coupling yields the shortest possible path for the gas transfer from the sample to the MS. An intense, highly parallel molecular beam is collimated by the aerodynamic beam *SKIMMER* from the barrel-shaped jet expansion behind the divergent nozzle. The pressure reduction of the purge gas flow at atmospheric pressure down to the high vacuum behind the *SKIMMER* orifice is achieved in two steps along a distance of less than 20 mm. All components are heated to at least the sample temperature and therefore there is little chance for condensation; even metal vapors are detected by this unrivaled coupling system.

The nozzle and *SKIMMER* are precisely machined from either alumina or amorphous carbon (glassy carbon), allowing application temperatures of 1450°C or 1950°C in the corresponding furnaces. The molecular beams are analyzed by a quadrupole mass spectrometer up to high mass numbers of 512 amu.

STA 449 ***F3*** *Jupiter*® with *SKIMMER* furnace

GC-MS Coupling

Mass spectrometer | Gas chromatograph | STA 509 *Jupiter®*

Gas chromatography (GC) is a method for separation of volatile and semi-volatile compounds with high resolution. Gas mixtures are separated based on the differences in component distribution between a stationary phase (e.g., inner coating of a capillary) and a mobile phase (purge gas, e.g., He, N, Ar, H_2).

Gas components with low affinity for the stationary phase but higher affinity for the mobile phase will be rapidly carried away by the purge gas, whereas gases with a high affinity for the stationary phase will follow with a relatively significant time delay ("retention time").

The mobile phase in GC is a gas, therefore all analytes must be evaporated and introduced into the column in gas form. The stationary phase in the GC is for universal applications. In current technology, this is usually a polymeric coating inside a long and narrow fused silica capillary.

MS is applied as a detection system at the outlet of the GC separation column and will register the time distribution of the separated gas components in the purge gas flow. This pre-separation of gases by the GC, along with the sensitivity and resolution of the MS, provide detailed structural information on most compounds and thus allow for their precise identification. The GC-MS can be coupled to any of the NETZSCH STAs via a heated transfer line.

Some of the GC-MS specifications are summarized below.

Technical Data	
Mode/Ionization	Non-coated inert source, electron impact ionization (EI)
Transfer line temperature	100°C to 300°C
Furnace adapter head temperature	max. 300°C
Mass filter	Monolithic hyperbolic quadrupole
Mass range	1.6 amu to 1050 amu
Mass resolution	Unit mass, adjustable
Valve box	Heatable up to 300°C, Sampling loop 250 µl

Applications

Thermal Conductivity

Thermal Conductivity of Four Stoichiometric Oxide Ceramics

Depicted here is the thermal conductivity of four stoichiometric oxide ceramics with 95% to 98% theoretical density. The materials show the classical trends for non (or low) electrical conductors. That is, exponential and 1/T decay with increasing temperature due to defect and phonon-phonon scattering, respectively. Further, decreasing thermal conductivity with increasing difference in ion mass is typical, that is:

$\lambda_{UO_2} < \lambda_{ThO_2} < \lambda_{Al_2O_3} < \lambda_{BeO}$.

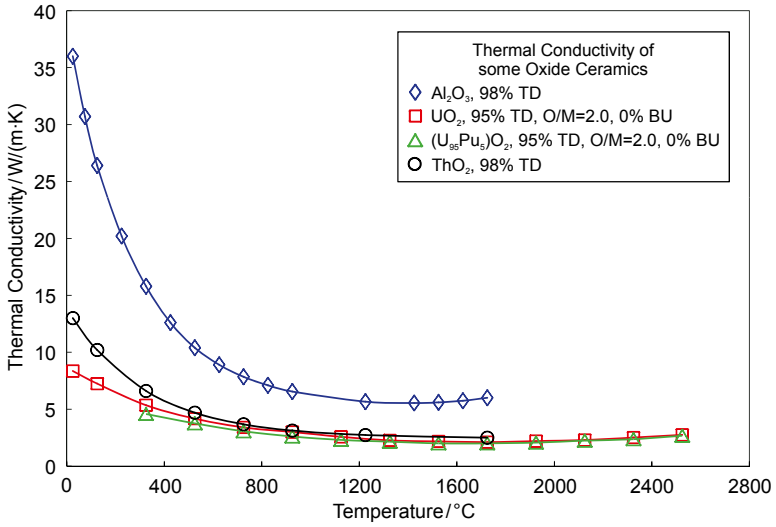

Thermal Conductivity of Some Actinide Nitrides

Increasing thermal conductivity with temperature indicates a significant electronic component and decreasing electrical resistivity. Decreasing thermal conductivity with increasing ion mass difference suggests increased phonon-electron scattering, i.e., shorter mean free path.

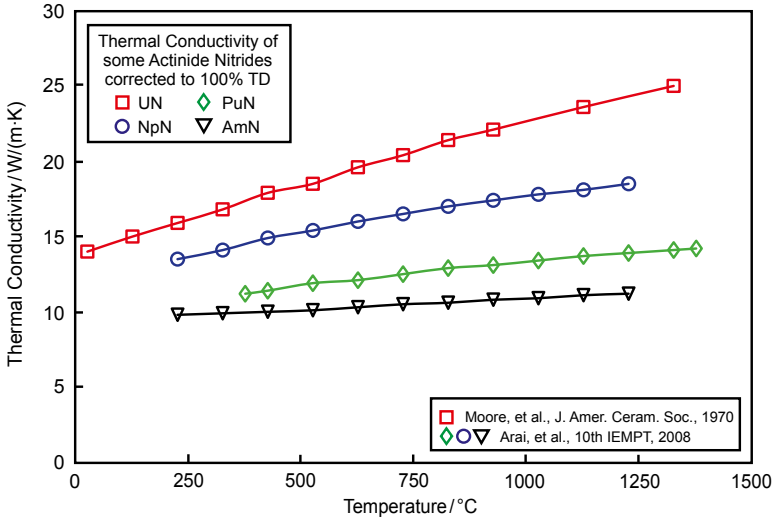

Thermal Conductivity of Three Carbide Ceramics

Even though a conductor, SiC follows the classical lattice thermal conductivity trend, while ZrC displays more of a dominant electronic trend. UC shows only a slight decrease in thermal conductivity with increasing temperature. This is due to the fact that the electronic and lattice component trends almost nullify each other even though the electronic component is dominant.

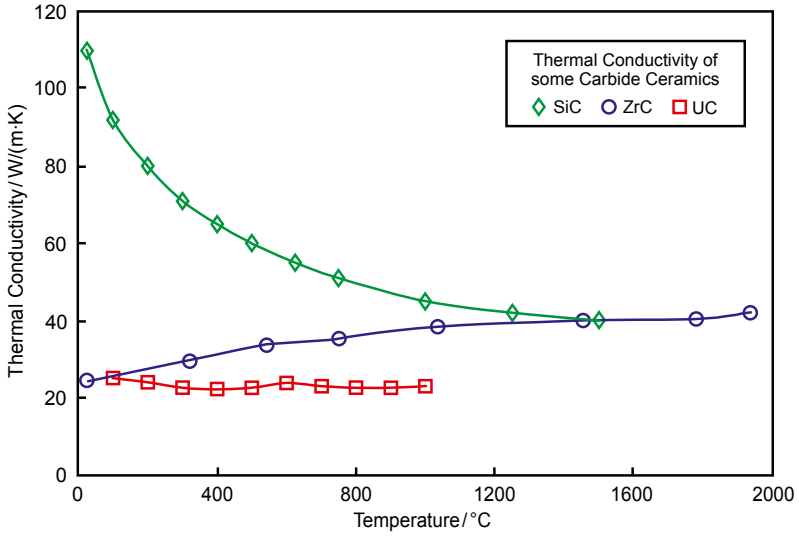

Thermal Conductivity of Uranium Nitride

In this example, the thermal conductivity of UN has been separated into the lattice and electronic components. Here the typical lattice 1/T and increasing electronic behavior is displayed. Note the noncoincidental agreement between the lattice thermal conductivities of UN and UO_2. It must be pointed out here that the lattice and electronic components of thermal conductivity were calculated from thermal conductivity and electrical resistivity measurements using a fitting routine. The Wiedemann-Franz-Lorenz (WFL) law, which can lead to significant errors in regions of non-elastic scattering, was not applied directly.

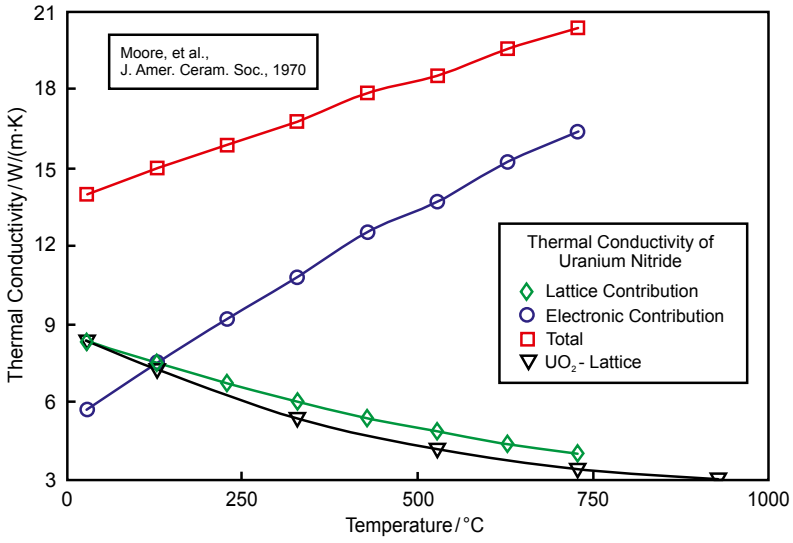

Specific Heat and Transition Energetics

Specific Heat of IN-718

The specific heat and heat of fusion of IN-718 up to ≈1450°C during heating and cooling are presented here. Integration of the melting peak yields ΔH≈185 J/g ±5.0%. The solidus and liquidus temperatures were also determined from these data. It should be noted however that care must be taken not to lose sight of possible undercooling, which is not atypical for metals. The solidus and liquidus temperatures are 1252°C and 1347°C, respectively.

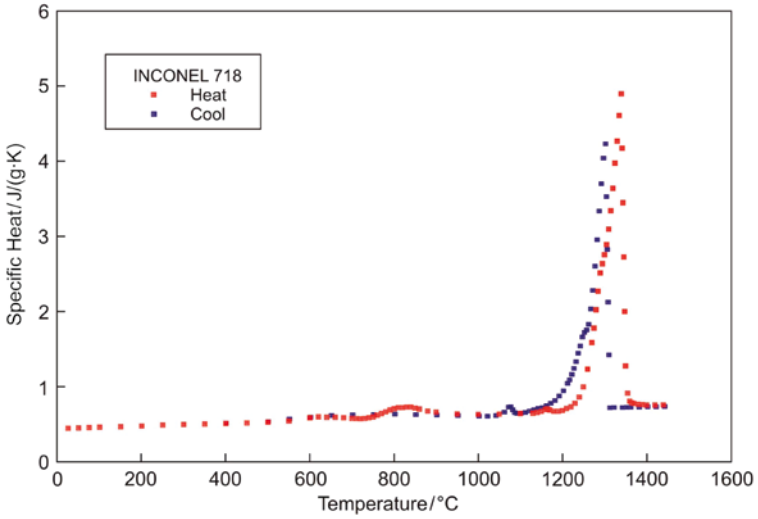

Specific Heat of Zr-40wt%U Metal Fuel

The specific heat of Zr-40wt%U fuel was measured between 25°C and 1000°C. Other than the endothermic peak between approximately 550°C and 620°C, which is due to the phase transition, the measured specific heat values are in reasonably good agreement with those calculated by the Neumann-Kopp rule.

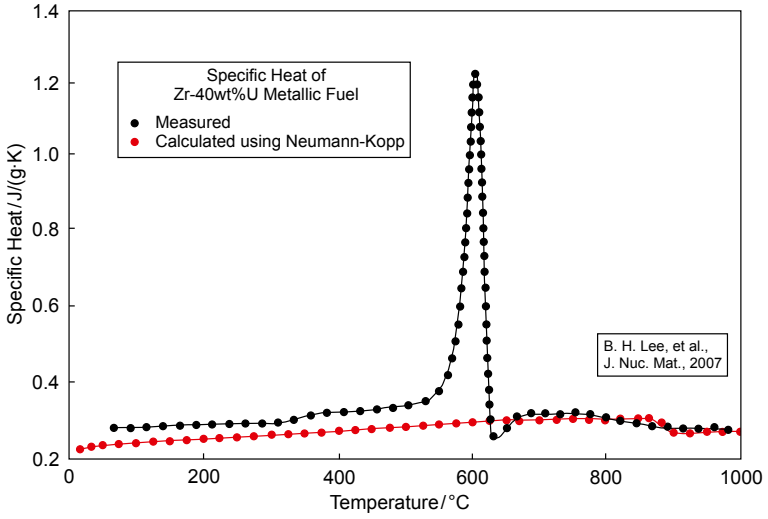

Thermal Expansion

Thermal Expansion of Some Thermal Neutron Absorbers

The thermal expansion of some ceramic and elemental neutron absorbers is presented here. In general, these materials expand somewhere between 1.0% and 3.0% between 25°C and the melting temperature. This is the expected behavior.

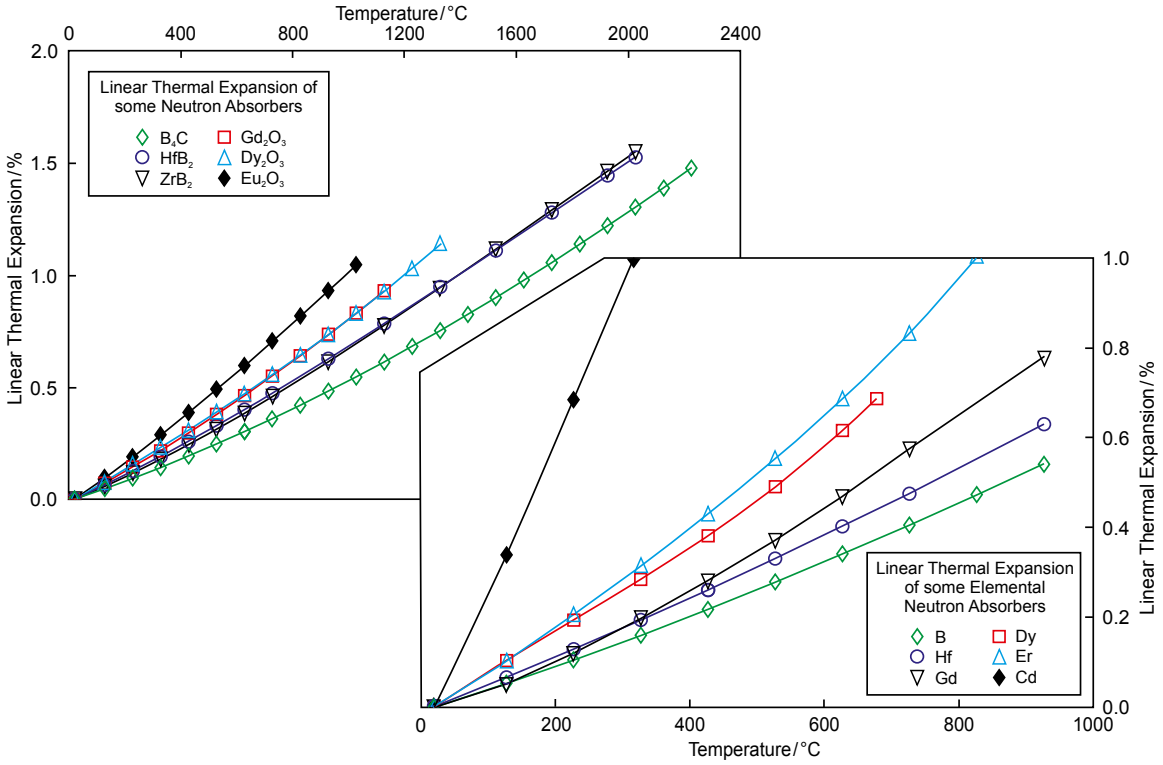

Thermal Expansion of Some Nitride Ceramics

In comparing the thermal expansion of several nitride ceramics, it is interesting to note that the thermal expansion increases with ion mass difference. This increasing asymmetric behavior is also responsible for increased phonon and phonon-electron scattering, resulting in shorter mean free paths and therefore inverse behavior between thermal expansion and thermal conductivity in many ceramics.

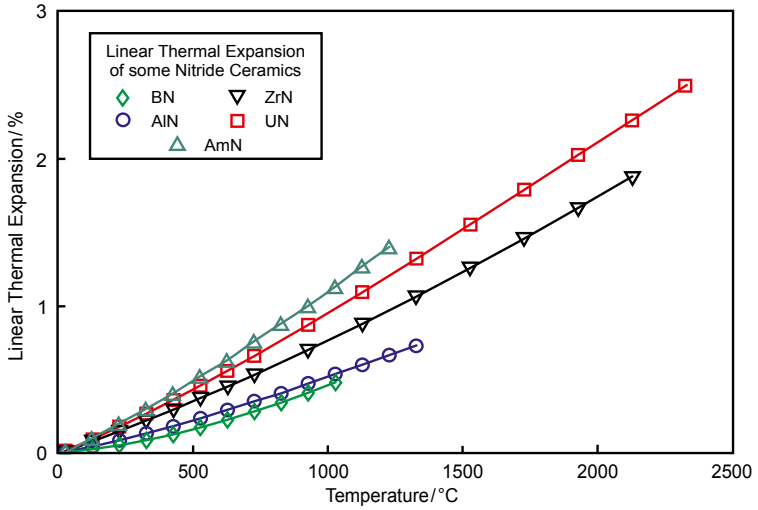

Urania

Mass Change of Hyperstoichiometric UO_2

Plotted are the mass change and rate of mass change in inert and reducing atmospheres. Clearly the curves overlay until ≈325°C. The first mass loss step below 325°C is due to the evolution of moisture and impurities. Above 325°C the curves deviate because of the greater oxygen loss in the reducing atmosphere. By 700°C the urania is stoichiometric in the reducing atmosphere, while in the inert atmosphere the material remains over-stoichiometric. This has far-reaching consequences with regard to the sinterability.

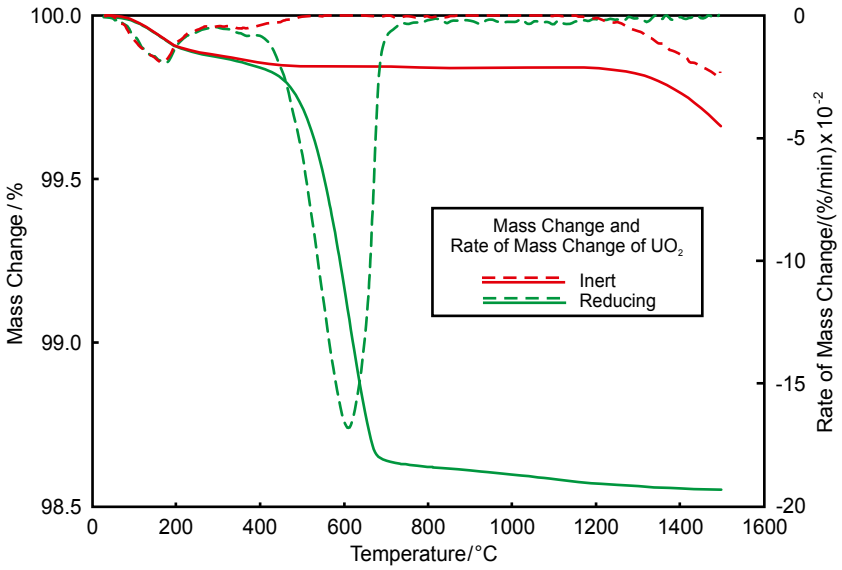

Oxidation of Stoichiometric UO_2 in an Air Atmosphere

The conversion from UO_2 to U_3O_7 to U_3O_8 is of course accompanied by mass increases of 1.14% and 1.72%. The exothermal energetics of the transitions are clearly shown by the DSC curve. It is interesting to note the excellent correlation between the mass change, rate of mass change and energetic curves. This plot clearly shows the advantage of simultaneous TG-DSC (STA) measurements using one instrument.

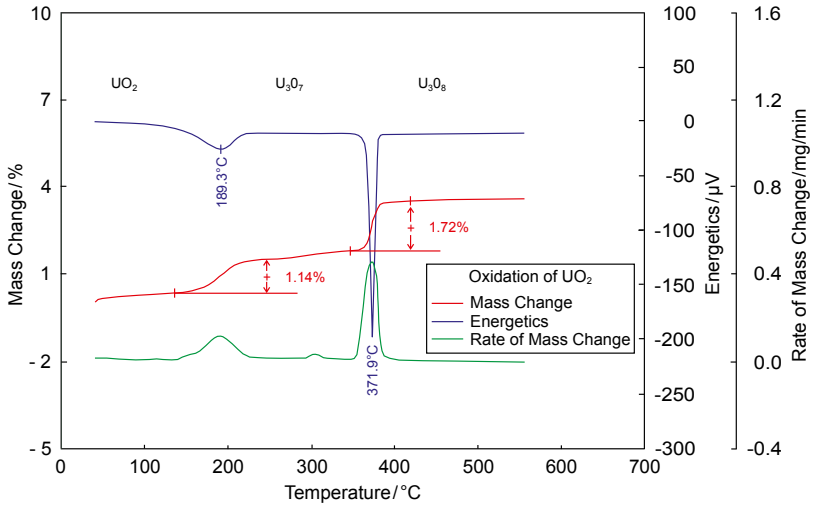

Specific Heat of UO_2

The specific heat of stoichiometric and overstoichiometric UO_2 are shown here. The stoichiometric UO_2 follows the classical temperature-dependent specific heat trend, while that for $UO_{2.04}$ and $UO_{2.084}$ display an endothermic peak between approximately 600 and 950K. This is due to energy required to dissolve the U_4O_9 phase. Notice that the peak area for $UO_{2.084}$ is larger than that for $UO_{2.04}$ because of the greater quantity of the U_4O_9 phase.

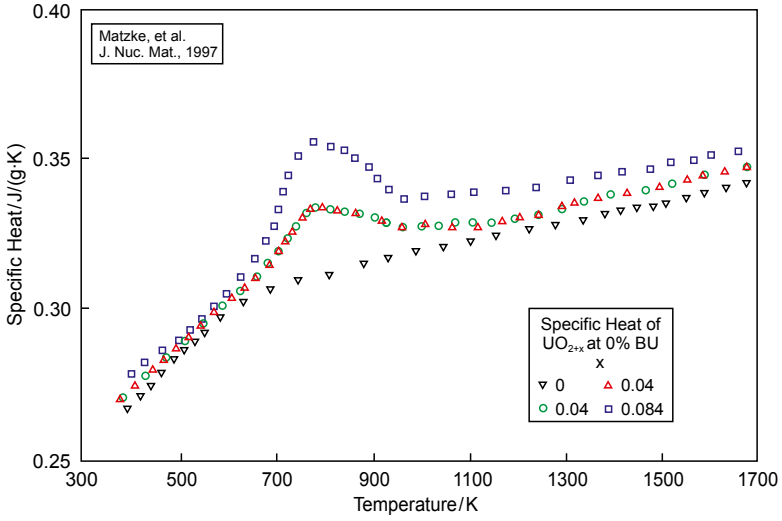

Thermal Diffusivity of UO_2

The thermal diffusivity of 95% dense stoichiometric UO_2 follows the expected 1/T behavior for lattice-driven transport at these temperatures. It should be noted that the thermal conductivity does not display this trend at temperatures above ≈2000K, because the specific heat does not follow the Debye theory.

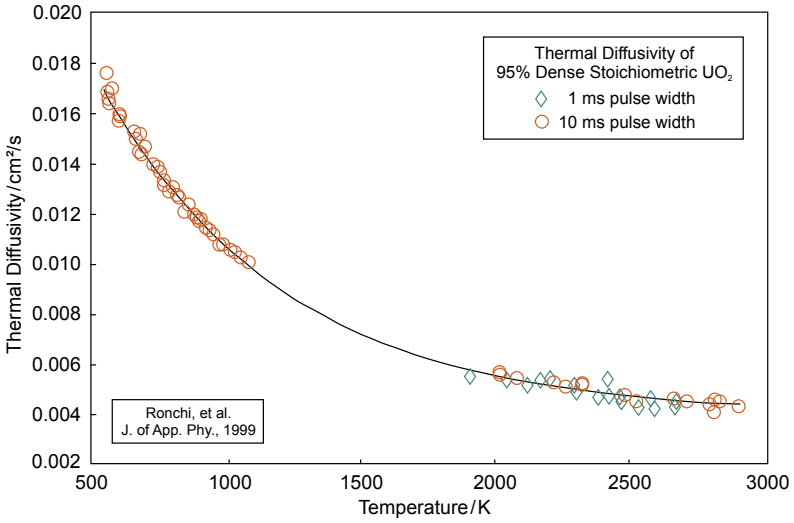

Thermal Diffusivity of $(U,Ce)O_{2-X}$

The thermal diffusivity of $(U,Ce)O_{2-X}$ follows the expected 1/T trend for lattice transport. Also, the impact of increased lattice strain (⇨ defect-phonon scattering) with increasing Ce content on thermal diffusivity is obvious.

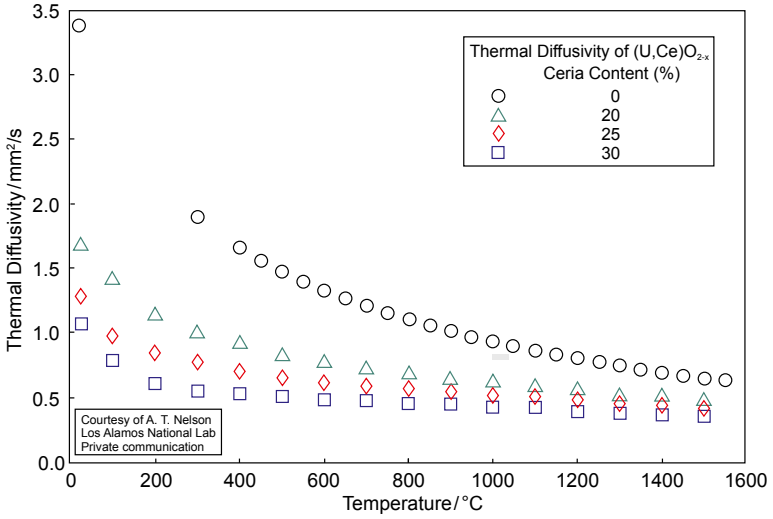

Inverse Thermal Diffusivity of $(U,Ce)O_{2-X}$

Here, the inverse thermal diffusivity $a^{-1} = A + B \cdot T$ (A and B represent defect-phonon and phonon-phonon scattering, respectively) is plotted against temperature and Ce content. As anticipated, this yields a series of curves with a relatively constant slope, B. The effect of solutionized Ce ions on defect-phonon scattering can be further quantified by plotting A against the Ce content.

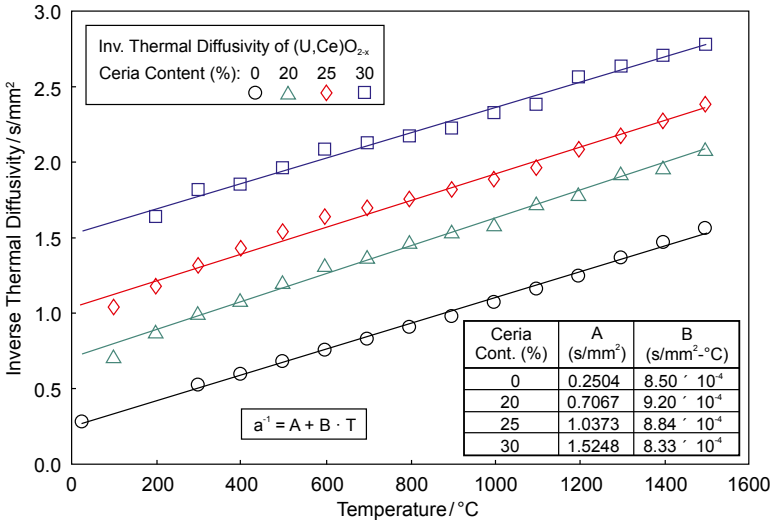

Ceria Cont. (%)	A (s/mm²)	B (s/mm²-°C)
0	0.2504	8.50 ´ 10⁻⁴
20	0.7067	9.20 ´ 10⁻⁴
25	1.0373	8.84 ´ 10⁻⁴
30	1.5248	8.33 ´ 10⁻⁴

Gadolinia

Sintering of Gadolinia

Shown here are the densification and rate of densification of $GdO_{1.5}$. The densification follows the expected heating rate and temperature dependence up to ≈1250°C. At ≈1250°C the heating rate dependence disappears and the rate of densification increases dramatically. This is due to the cubic to monoclinic phase transition, which significantly complicates the interpretation of the sintering data.

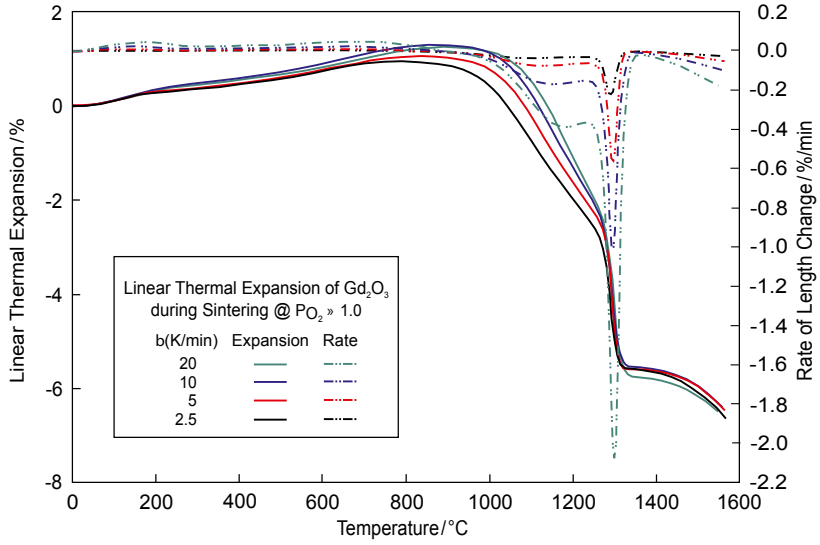

Specific Heat of Gadolinia

This plot depicts the specific heat of $GdO_{1.5}$ during the first (sintering) and second heatings. Clearly the phase transition, with a ΔH of ≈14.6 J/g, is irreversible. This has been verified by XRD data. The low temperature endothermic and exothermic trends in the first heating data are due to the release of moisture and other impurities.

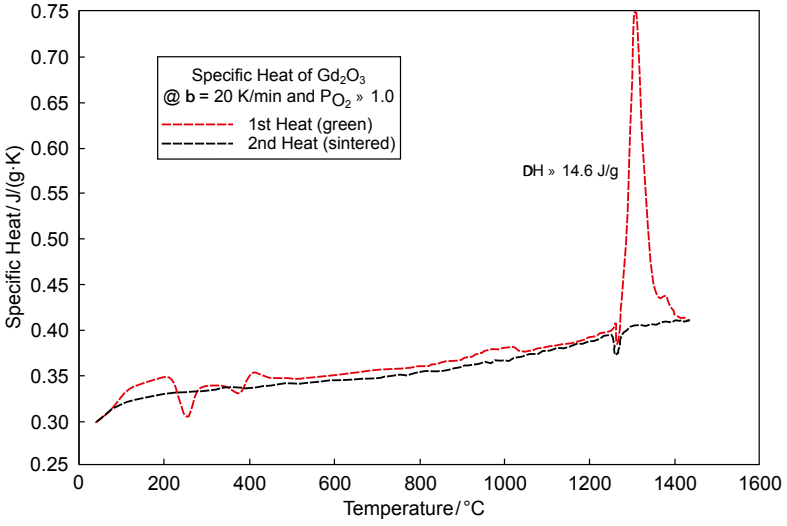

Ceria

Densification of CeO_2

The shrinkage and rate of shrinkage of ceria at five different heating rates during sintering are plotted here. The samples were pressed to 51-53% theoretical density at 355 MPa. No binders or mold lubricants were employed. The onset of densification occurs at ≈800°C and sintering is not complete by 1660°C. Typical heating rate dependence due to rate-limited metal atom diffusion is displayed. The curves show a two-step densification process which is somewhat atypical. Final density was 81-85% of theoretical.

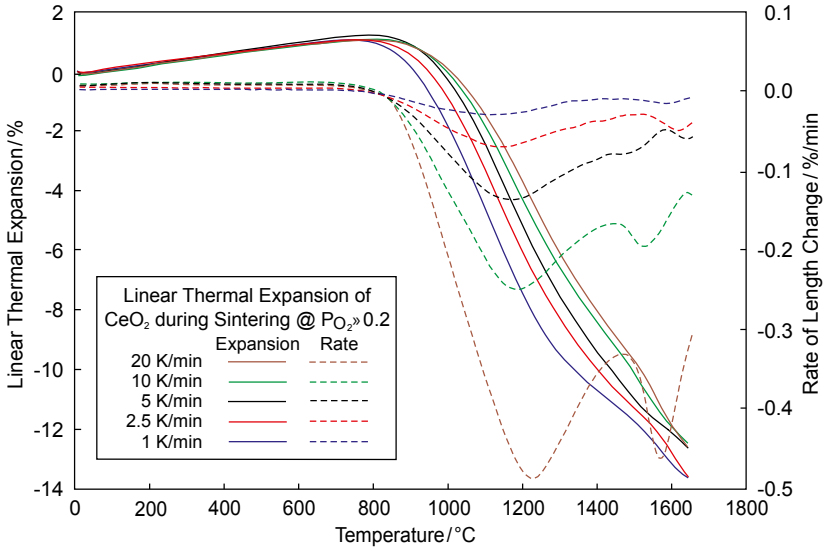

O/M Ratio of CeO_2 During Sintering

This figure shows the O/M ratio during heating. These values were calculated from TGA data measured under multiple partial pressures of oxygen (P_{O_2}). Sample preparation was identical to that above. During heating the O/M starts to decrease at ≈1000°C and there are clearly different reduction rates resulting from the variable P_{O_2} over the sample. The process is reversible. The resulting deviation from stoichiometry has a profound effect on the sinterability.

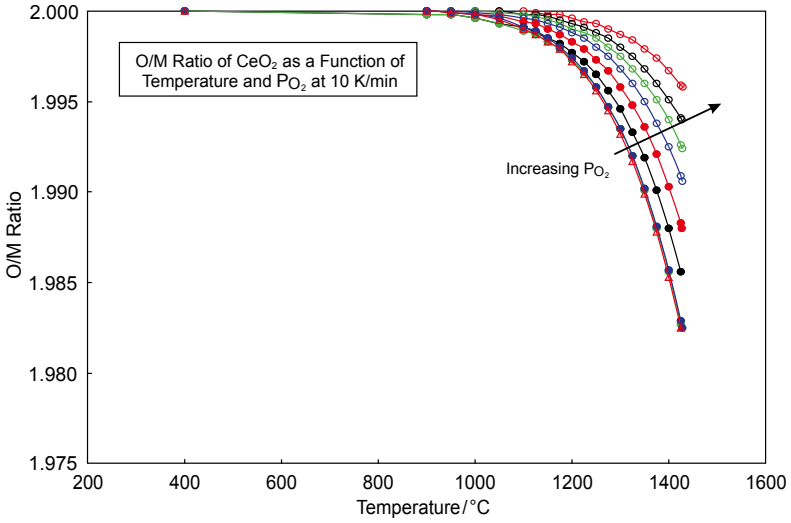

Specific Heat of CeO_2 During Sintering

Depicted here is the specific heat of ceria with and without reduction. Sample preparation remained unchanged. In the absence of reduction the specific heat follows the Debye theory and is in good agreement with published values. With reduction the specific heat (actually apparent specific heat) increases non-linearly with temperature. This is a result of the energy required for the increased rate of defect formation. The reduction becomes obvious at ≈950°C. The difference between the two curves is often referred to as the excess specific heat.

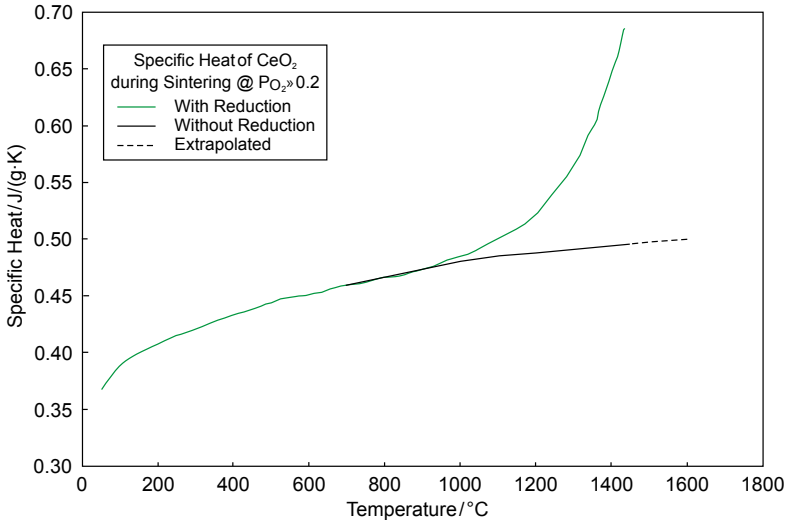

Property Evolution of CeO_2 During Sintering

In this figure the thermal diffusivity, specific heat, bulk density, rate of change of bulk density and O/M are superimposed. First, the correlation between the specific heat and O/M is obvious. Next, the thermal diffusivity increases between ≈400°C and 850°C due to surface diffusion (no densification). The increase in thermal diffusivity above ≈850°C is a result of decreasing porosity (densification), but is partially attenuated by the decreasing O/M (increased defect scattering). The densification (diffusion) rate between O/M=1.9995 and 1.9840 (1165°C and 1620°C) is controlled, in part, by the O/M-created defects. Likely controlling mechanisms are $V_M \rightarrow M_i$ /cluster. XRD measurements show that above ≈1600°C coarsening occurs at the expense of densification, which manifests itself as a drop in the sintering rate.

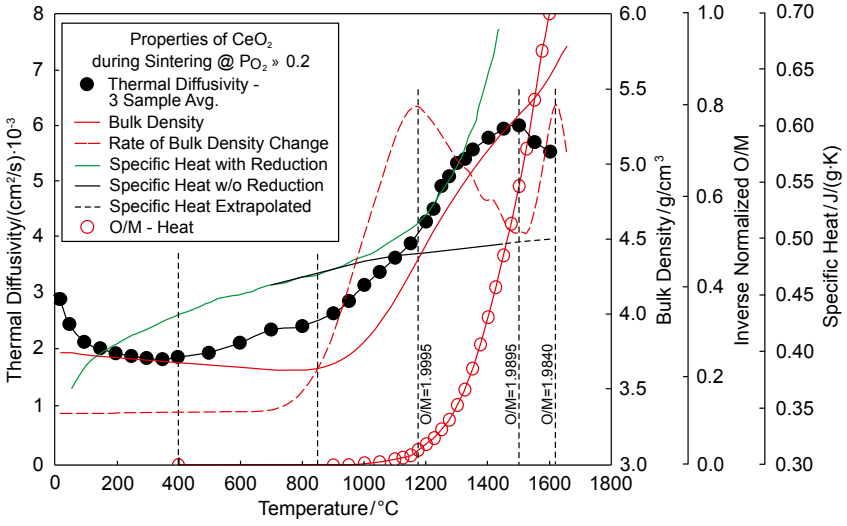

Graphite

Specific Heat of Graphite

The specific heat of graphite was measured over the temperature range of -100°C to 1300°C. As expected, the trend follows the Debye theory (electronic specific heat is negligible at these temperatures). The measured and published values deviate by a maximum of ≈5.0% and are generally within ≈2.0%. Note the reproducibility of the measurements over both the low-temperature (LT) and high-temperature (HT) ranges.

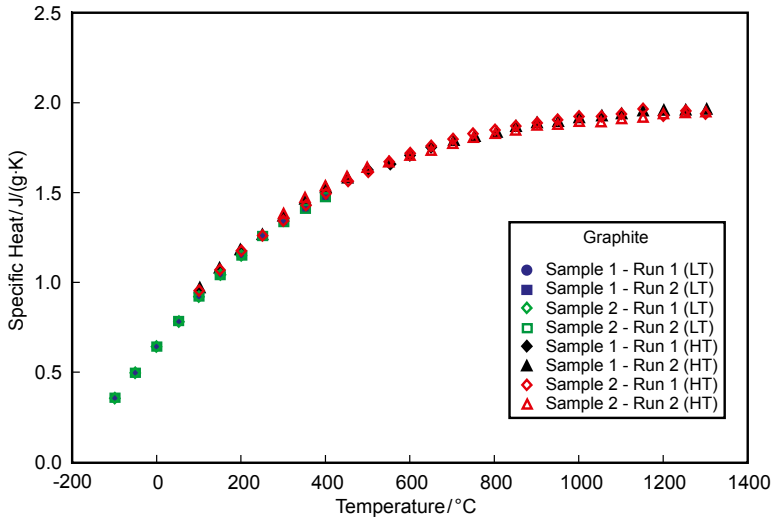

Thermal Expansion of POCO Graphite

The thermal expansion of high-purity POCO graphite was measured over the temperature range of 500°C to 2800°C. Clearly the reproducibility is excellent and, as shown, the deviation from literature values is significantly less than 1.0%.

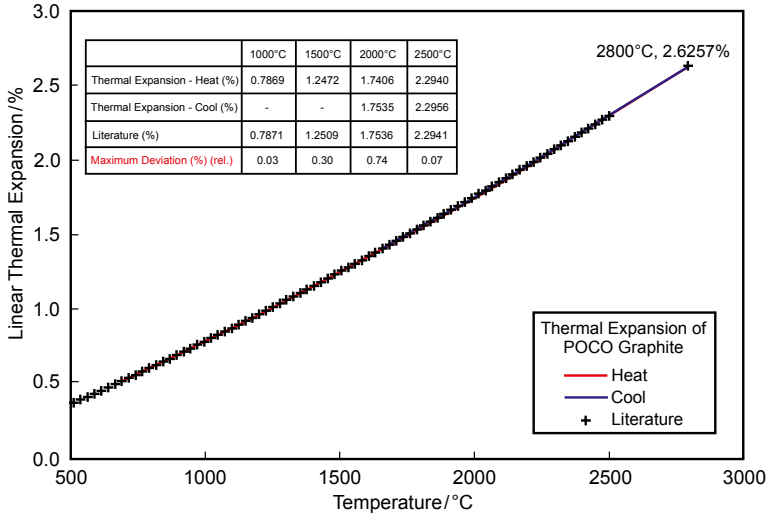

	1000°C	1500°C	2000°C	2500°C
Thermal Expansion - Heat (%)	0.7869	1.2472	1.7406	2.2940
Thermal Expansion - Cool (%)	-	-	1.7535	2.2956
Literature (%)	0.7871	1.2509	1.7536	2.2941
Maximum Deviation (%) (rel.)	0.03	0.30	0.74	0.07

Stored Energy in Graphite

Here the apparent specific heat curves for irradiated graphite are superimposed on those for the true specific heat of unirradiated graphite. As expected, the lower irradiation temperature, T_{irr}, results in more stored energy because fewer defects are annealed out. Of course, once T_{irr} is exceeded stored energy is released, resulting in a decrease in the apparent specific heat.

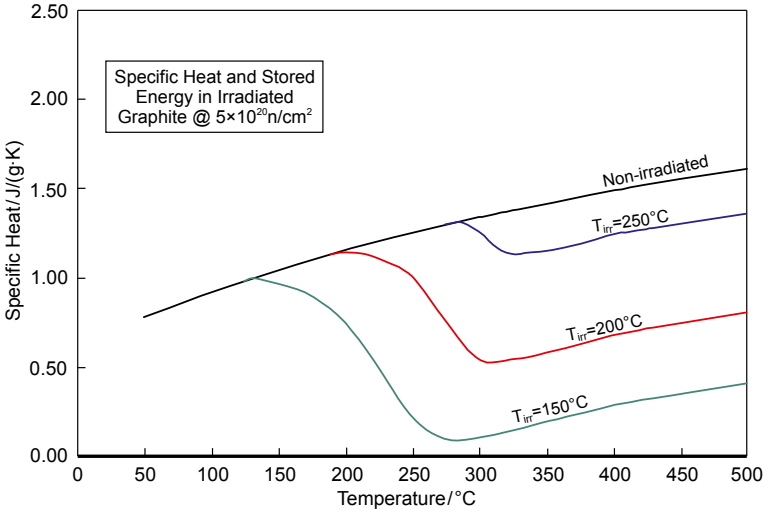

Thermal Diffusivity and Thermal Conductivity of Graphite

The thermal diffusivity of graphite was measured over the temperature range of 25°C to about 2800°C. The thermal conductivity was calculated using the measured specific heat, bulk density and thermal diffusivity data. The calculated thermal conductivity follows the expected 1/T behavior for graphite.

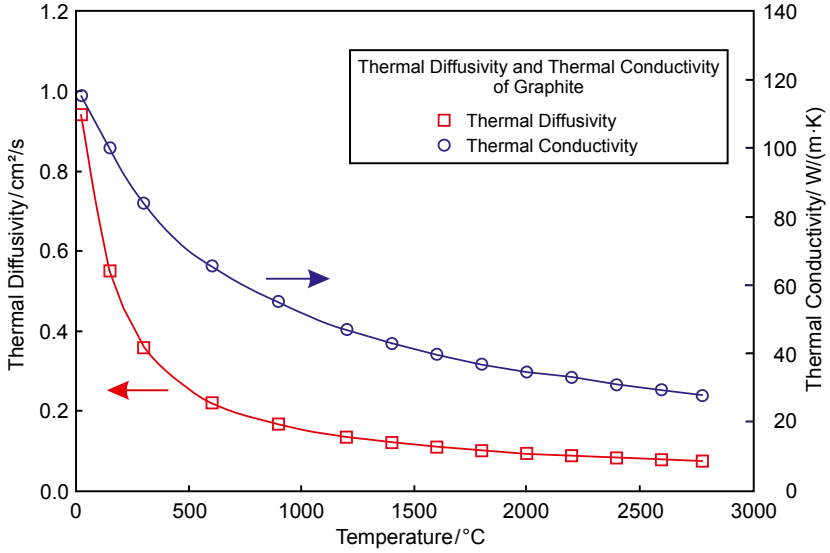

Cladding

Oxidation of Zircaloy-4

Presented here are the mass gain and detected H_2 during oxidation of Zircaloy-4 cladding in a steam atmosphere. The oxidation is due, of course, to the highly exothermic reaction $Zr + 2H_2O \rightarrow ZrO_2 + 2H_2 + \Delta H$.

The heating rate dependence of the oxidation and therefore the H_2 production is obvious. At the 5 K/min heating rate the rate of mass gain and H_2 production reach steady-state at approximately 950°C, which is not the case for the faster 10 K/min rate.

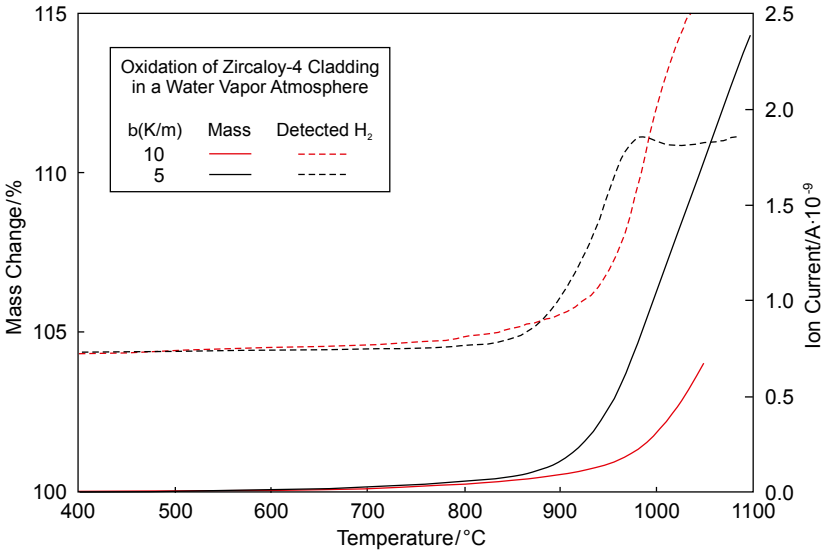

Heat Flow in a Zirconium Alloy

The heat flow during heating and cooling in a Zr-Nb alloy over the temperature range of 400°C to ≈1050°C has been analyzed. Of interest here is the solid-solid endothermal phase transition between ≈815°C and 990°C on heating. Upon cooling, the exothermal phase transition is shifted to lower temperatures, i.e. between ≈985°C and 750°C. Notice that the transition energetics are relatively equal at 47.4 J/g and 47.5 J/g on heating and cooling, respectively. This is not atypical for stable metal alloys.

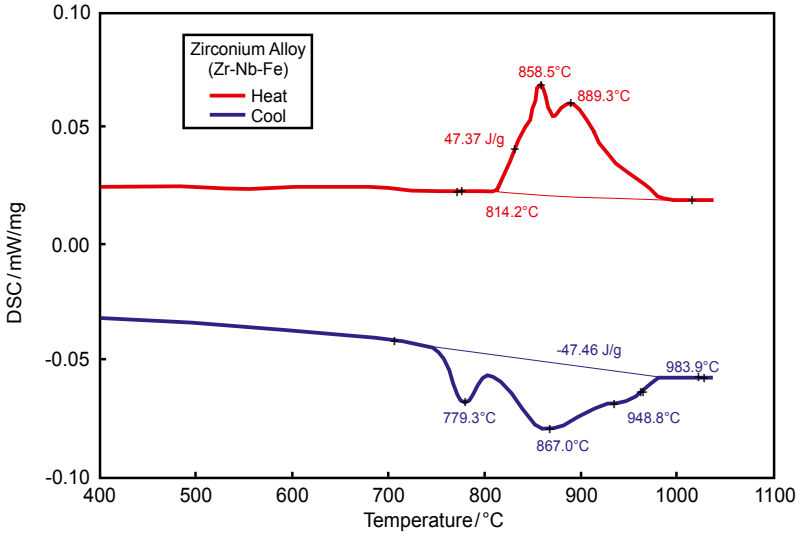

Waste Surrogates

Thermal Diffusivity and Specific Heat of a Waste Glass

The thermal diffusivity and specific heat of a waste glass consisting of oxides ranging from alumina to neodymia are plotted here. The specific heat data show the glass transition (endothermal) in the range of 500°C followed by cold crystallization (exothermal) between 600°C and 750°C, indicating that the sample was cooled fast enough to produce a significant amorphous phase. Also, the large excess enthalpy peak superimposed on the glass transition may indicate significant aging time below the transition. The diffusivity displays the classical 1/T behavior followed by a significant drop across the glass transition. The correlation between the two data sets is excellent.

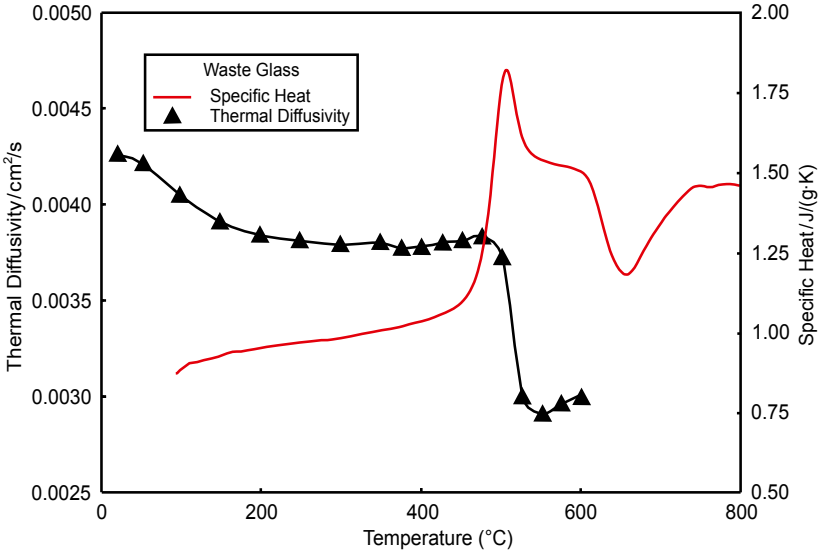

Evolved Gas Measurement on Surrogate Waste Material

Waste material can contain silicates like clays contaminated with radioactive inorganic salts (hydrates, sulphates, nitrates etc.). The processing of these waste materials is often done by a heat treatment. TG-MS measurements allow the determination, identification and quantification of the evolved gases during heating of these materials. The surrogate material for this investigation contained vermiculite and alkali and earth alkali nitrates. During linear heating at 10 K/min in a He atmosphere, water, nitrogen oxide, nitrogen dioxide and carbon dioxide were detected. The water came off between RT and about 400°C, nitrogen dioxide shows two intensity maxima at about 180°C and 497°C. The nitrogen oxide emission starts at around 300°C and shows maximum intensity at 668°C. The amount of CO_2 is very small. Most probably there are some impurities of organic material, hydrocarbons or carbonates. Even during storage in an air atmosphere some carbonates could be formed due to the small grain size of the material.

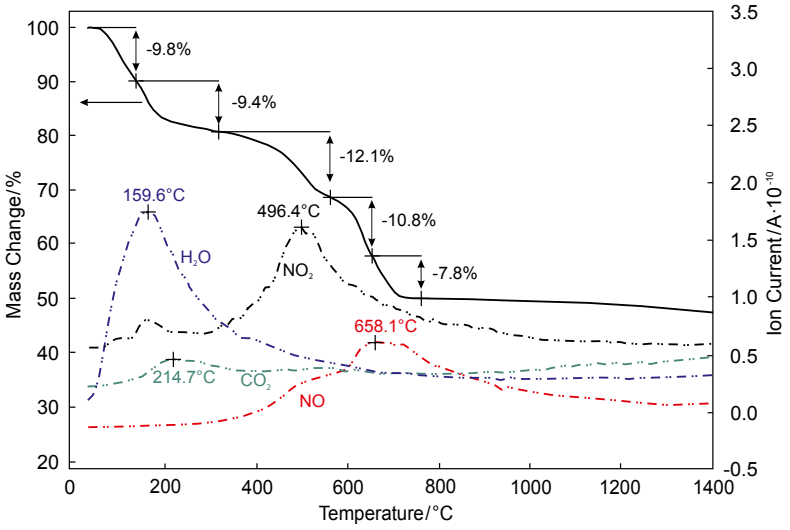

Thermophysical Properties

of Some Important Nuclear Materials

The properties given in this table are intended to be used as estimates only. Some are quite accurate while others are less certain. Of course it is well known that small changes in stoichiometry, porosity, microstructure, etc. can have a profound effect on the thermophysical properties. As a result, NETZSCH does not guarantee the accuracy of these values.

Fuels

Material	Property		
	λ [W/(m·K)]	C_p [J/(g·K)]	ρ [g/cm³]
Pu	6.7	0.145	19.816
PuC	6.9	0.176	-
PuN	9.6	-	14.400
PuO_2	6.3	0.240	11.460 th.
Th	54.0	0.118	11.700
ThO_2	13.0	0.235	9.110 th.
U	27.6	0.116	19.070
U-14%Zr	18.5	-	-
U-91%Zr	7.4	-	-
$(U_{0.8}\ Pu_{0.2})O_2$	8.9 @ th.	0.240	11.660 th.
UC	25.3	0.200	13.630 th.
UN	13.0	0.190	14.300 th.
UO_2	8.7 @ th.	0.235	10.960 th.

Miscellaneous

Material	Property		
	λ [W/(m·K)]	C_p [J/(g·K)]	ρ [g/cm³]
Al_2O_3	36.0	0.765	3.970
MgO	60.0	0.929	3.770
Si_3N_4	16.0	0.691	2.700
SiC	120.0	0.675	3.160
ZrC	26.3	0.378	6.730
ZrN	10.5 (80-90%th.)	0.386	7.090
ZrO_2 (Y-stab.)	1.9	0.455	5.680

Structural

Material	Property		
	λ [W/(m·K)]	C_p [J/(g·K)]	ρ [g/cm³]
InX-750	11.7	0.439	8.510
Low Cr Steel	42.3	0.442	7.858
Nichrome	12.0	0.420	8.400
SS-304	14.9	0.477	7.900
SS-316	13.4	0.468	8.238
Zirc2	17.0	0.290	6.550
Zirc4	14.1	0.293	6.580
Zr-2.5%Nb	19.0	0.315	6.570

at Room Temperature

Additional elements			
Material	Property		
	λ [W/(m·K)]	C_p [J/(g·K)]	ρ [g/cm³]
Ag	429.0	0.235	10.500
Al	237.0	0.903	2.702
Cd	96.6	0.231	8.650
Ce	11.3	0.192	6.770
Cr	93.7	0.449	7.160
Fe	80.2	0.447	7.870
In	81.8	0.267	7.310
Mg	156.0	1.024	1.740
Mo	138.0	0.251	10.240
Nb	53.7	0.265	8.570
Ni	90.7	0.444	8.900
V	30.7	0.489	6.100
W	174.0	0.132	19.300
Zr	22.7	0.278	6.570

Miscellaneous			
Material	Property		
	λ [W/(m·K)]	C_p [J/(g·K)]	ρ [g/cm³]
Be	200.0	1.825	1.850
BeO	270.0	1.030	3.000
D_2O	0.560	4.230	1.100
Graphite	100.0	0.710	1.700
H_2O	0.561	4.217	1.000
$ZrH_{1.8}$	34.0	0.410	5.620

Structural			
Material	Property		
	λ [W/(m·K)]	C_p [J/(g·K)]	ρ [g/cm³]
AgInCd	60.0	0.230	10.170
B	27.0	1.107	2.500
B4C	92.0	0.960	2.520
BN	28.7	0.848	2.250
Hf	22.3	0.363	13.090
HfB_2	22.6	0.396	11.200
Ta	57.5	0.140	16.600
ZrB_2	23.0	0.230	6.090

sources: diverse

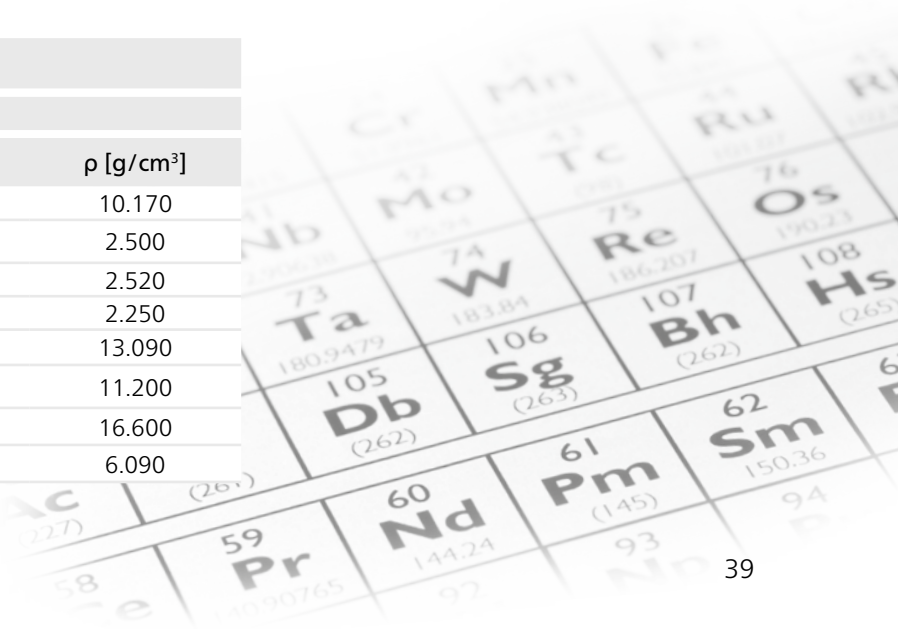

Expertise in Service

Our Expertise – Service

All over the world, the name NETZSCH stands for comprehensive support and expert, reliable service, before and after sale. Our qualified personnel from the technical service and application departments are always available for consultation.

In special training programs tailored for you and your employees, you will learn to tap the full potential of your instrument.

To maintain and protect your investment, you will be accompanied by our experienced service team over the entire life span of your instrument.

Summary of Our Services

- Installation and commissioning
- Hotline service
- Preventive maintenance
- On-site repairs with emergency service for NETZSCH components
- Moving / exchange service
- Technical information service
- Spare parts assistance

R&D and Engineering

Our R&D and Engineering teams are regarded as some of the world's finest. NETZSCH employs the largest number of PhD engineers, physicists, material scientists and chemists in the industry. Our philosophy is to continuously expand the boundaries of technology, ensuring that our instruments lead the world in performance, quality and robustness. This is proven by the longevity of our instruments as well as the many patented and proprietary features incorporated into them.

For the nuclear industry, we engineer special instruments for glovebox and hot cell applications in addition to our standard products. We utilize mock-up gloveboxes throughout the design and construction processes to ensure that our instruments can be serviced and operated efficiently in these rigorous environments. Further, we access mock-up hot cell facilities to give us the experience required to produce instruments which are robust enough to be handled efficiently in the even more demanding hot cell environments.

We invite you to join us at our headquarters in Selb, Germany to work together on an instrument solution for your specific application and hot environment. For your convenience, our nuclear applications specialists and engineers are also available to work with you on site at your facility.

At NETZSCH, we convert the impossible to reality – challenge us.

Our Expertise

Our Expertise – Applications Laboratories

The NETZSCH Thermal Analysis Applications Laboratories are a proficient partner for thermal analysis issues. Our involvement in your projects begins with painstaking sample preparation and continues through meticulous examination and interpretation of the measurement results. Our measuring methods are state-of-the-art.

Customers of our laboratory services stem from a wide range of large companies in industries such as chemical, automotive, electronics, air/space travel, racing, and polymer and ceramics.

Commercial Testing

Within the realm of thermal analysis and thermophysical properties, we offer you a comprehensive line of the most diverse thermal analysis techniques for the characterization of materials (solids, powders and liquids). Measurements can be carried out on samples of the most varied of geometries and configurations.

Consult with the experts in our applications laboratories to choose the best-suited measuring method for your specific needs.

You will be working with scientists (physicists, chemists, materials scientists) possessing consolidated knowledge about the most varied of methods and materials spectra.

Notes

The owner-managed NETZSCH Group is a leading global technology company specializing in mechanical, plant and instrument engineering.

Under the management of Erich NETZSCH B.V. & Co. Holding KG, the company consists of the three business units Analyzing & Testing, Grinding & Dispersing and Pumps & Systems, which are geared towards specific industries and products. A worldwide sales and service network has guaranteed customer proximity and competent service since 1873.

When it comes to Thermal Analysis, Calorimetry (adiabatic & reaction), the determination of Thermophysical Properties, Rheology and Fire Testing, NETZSCH has it covered. Our 60 years of applications experience, broad state-of-the-art product line and comprehensive service offerings ensure that our solutions will not only meet your every requirement but also exceed your every expectation.

Proven Excellence.

NETZSCH-Gerätebau GmbH
Wittelsbacherstraße 42
95100 Selb, Germany
Tel.: +49 9287 881-0
Fax: +49 9287 881-505
at@netzsch.com
https://analyzing-testing.netzsch.com

NETZSCH®

www.netzsch.com

NGB · Characterization of Nuclear Materials · EN · 0725 · Technical specifications are subject to change.